

B-CONCORD - A scalable Bayesian high-dimensional precision matrix estimation procedure

Peyman Jalali, Kshitij Khare and George Michailidis

University of Florida

Abstract

Sparse estimation of the precision matrix under high-dimensional scaling constitutes a canonical problem in statistics and machine learning. Numerous regression and likelihood based approaches, many frequentist and some Bayesian in nature have been developed. Bayesian methods provide direct uncertainty quantification of the model parameters through the posterior distribution and thus do not require a second round of computations for obtaining debiased estimates of the model parameters and their confidence intervals. However, they are computationally expensive for settings involving more than 500 variables. To that end, we develop B-CONCORD for the problem at hand, a Bayesian analogue of the CONVex CORrelation selection method (CONCORD) introduced by Khare et al. (2015). B-CONCORD leverages the CONCORD generalized likelihood function together with a spike-and-slab prior distribution to induce sparsity in the precision matrix parameters. We establish model selection and estimation consistency under high-dimensional scaling; further, we develop a procedure that refits only the non-zero parameters of the precision matrix, leading to significant improvements in the estimates in finite samples. Extensive numerical work illustrates the computational scalability of the proposed approach vis-a-vis competing Bayesian methods, as well as its accuracy.

1 Introduction

Graphical models capture conditional dependence relationships between a set of random variables Bühlmann and Van De Geer [2011]. The emergence of high dimensional data, wherein researchers have measured a large number of variables p on a relative small number of samples n led to the study of estimating such models under *sparsity* constraints, namely that the number of true non-zero parameters is less than the sample size. A rich body of work on algorithms and the associated theoretical considerations emerged addressing this problem Wainwright [2019]. A key development was the introduction of the neighborhood selection method Meinshausen and Bühlmann [2006] which for Gaussian graphical models leverages the connection between the $(i, j)^{th}$ entry of the precision matrix $\mathbf{\Omega} = \mathbf{\Sigma}^{-1}$ -the model parameter of interest- to the partial correlation between the i^{th} and j^{th} variable; the

latter can be estimated through a regression model even under sparsity constraints. This regression approach was used for graphical models for binary variables, as well as mixed measurement variables (e.g. numerical, binary, count) Chen et al. [2015], in addition to the Gaussian case.

As previously mentioned, numerous approaches have been developed for estimation of a sparse precision matrix, either based on the neighborhood selection idea or leveraging the Gaussian likelihood; e.g., see Meinshausen and Bühlmann [2006], Yuan and Lin [2007], Friedman et al. [2008], Peng et al. [2009], Cai et al. [2011], Khare et al. [2015] and references therein. These approaches come with statistical guarantees expressed in the form of high probability error bounds for selecting the correct non-zero model parameters and for the norm difference between the estimated model parameters and the data generating ones. The Bayesian paradigm provides comprehensive uncertainty quantification of the model parameters through the posterior distribution. To that end, several Bayesian counterparts to the penalized (Gaussian) likelihood based methods have been proposed in the literature; e.g., see Dobra et al. [2011], Wang et al. [2012], Cheng and Lenkoski [2012], Wang [2015]. However, a key challenge for these approaches is their scalability to settings involving a large number of variables (e.g. $p \geq 500$).

The main goal of this paper is to develop a highly *scalable* Bayesian approach for sparse precision matrix estimation in high-dimensional settings with thousands of variables by leveraging the neighborhood selection method. This is accomplished by leveraging the regression based generalized likelihood function in Khare et al. [2015] and combined with a spike-and-slab prior distribution on the precision matrix $\mathbf{\Omega}$ parameters, to obtain a generalized posterior distribution. A key advantage of the generalized likelihood function is that the resulting posterior distributions for the elements of $\mathbf{\Omega}$ are available in closed form (up to a normalizing constant), unlike full Gaussian likelihood approaches. This enables derivation of a scalable Gibbs sampler that works well in settings involving thousands of variables (see numerical evidence in Section 4) and outperforms state of the art approaches in the literature. Further, we establish posterior consistency both for selecting the correct non-zero elements of $\mathbf{\Omega}$ and for the norm difference between the estimated model parameters and the data generating ones. In addition, to improve estimation accuracy of the magnitude of the non-zero elements in small sample settings, we introduce a novel refitting procedure with a modified prior distribution that achieves this objective, a novel development of independent interest for Bayesian methods for high-dimensional sparse estimation problems.

The remainder of the paper is organized as follows. The problem formulation based on the generalized likelihood function and the spike-and-slab prior distribution, together with the development of a scalable Gibbs sampler for sampling from the resulting posterior distribution is presented in Section 2. The novel refitting procedure is discussed in Section 2.2. High-dimensional selection consistency and convergence rates for the model parameters are established in Section 3. Extensive numerical evaluation of the proposed algorithm and an illustration to a Omics data set is given in Section 4. Finally, the proofs of all technical results and some background on the generalized likelihood function are delegated to the Appendix.

2 The Bayesian CONCORD (B-CONCORD) framework for precision matrix estimation

The key building block in the proposed framework is the CONCORD generalized likelihood function introduced in Khare et al. [2015] that is motivated by the regression based neighborhood regression approach for estimation of Gaussian graphical models introduced in Meinshausen and Bühlmann [2006] (*a brief introduction and derivation of it is given in Supplemental Section S 5*). Let $\mathcal{Y} := (\{\mathbf{y}_i\}_{i=1}^n)$ be independent and identically distributed observations from a p -variate (continuous) distribution, with mean $\mathbf{0}$ and covariance matrix $\mathbf{\Omega}^{-1}$. Then, the CONCORD generalized likelihood function is defined as follows.

$$\mathcal{L}_{CONCORD}(\mathbf{\Omega}) := \exp \left(-\frac{1}{2} \sum_{j=1}^p \sum_{i=1}^n \left(\omega_{jj} y_{ij} + \sum_{k \neq j} \omega_{jk} y_{ik} \right)^2 + n \sum_{j=1}^p \log \omega_{jj} \right). \quad (2.1)$$

Similarly to the neighborhood selection approach, for computational reasons we require that $\mathbf{\Omega} \in \mathbb{M}_p^+$, the space of real $p \times p$ symmetric matrices with positive diagonal elements, but *not* necessarily positive definite.

A Spike and Slab Prior Distribution for B-CONCORD.

For every off-diagonal entry of $\mathbf{\Omega} \in \mathbb{M}_p$, we assume the following: particular

$$\omega_{jk} \sim (1 - q) I_{\{0\}}(\omega_{jk}) + q \phi_{\lambda_{jk}}(\omega_{jk}) I_{\mathbb{R} \setminus \{0\}}(\omega_{jk}) \quad (2.2)$$

independently for every $1 \leq j < k \leq p$, where ϕ_λ denotes the normal density with mean zero and variance $1/\lambda$. Further, we impose an independent Exponential(γ) prior distribution on all the diagonal entries of $\mathbf{\Omega}$. Hence, the (shrinkage) hyperparameters are $\{\lambda_{jk}\}_{1 \leq j < k \leq p}$ and γ . We will discuss the choice of these hyperparameters in Remark 1.

We now introduce additional notation for ease of exposition, in particular for the asymptotic analysis in Section 3. Let

$$\boldsymbol{\xi} = (\omega_{12}, \omega_{13}, \dots, \omega_{1,p}, \omega_{2,3}, \dots, \omega_{p-1,p}) \quad (2.3)$$

denote the collection of off-diagonal entries of the symmetric matrix $\mathbf{\Omega}$. Further, let $\mathbf{l} \in \{0, 1\}^{\binom{p}{2}}$ be a generic sparsity pattern for $\boldsymbol{\xi}$. There are $2^{\binom{p}{2}}$ such sparsity patterns. For example, when $p = 3$, there are $\binom{3}{2} = 3$ off-diagonal entries, and the $2^{\binom{3}{2}} = 8$ possible sparsity patterns in the off-diagonal entries are

$$\begin{aligned} & (0, 0, 0), (1, 0, 0), (0, 1, 0), (0, 0, 1) \\ & (1, 1, 0), (1, 0, 1), (0, 1, 1), (1, 1, 1). \end{aligned}$$

For every sparsity pattern \mathbf{l} , let $d_{\mathbf{l}}$ be the density (number of non-zero entries) of \mathbf{l} , and $\mathcal{M}_{\mathbf{l}}$ be the space where $\boldsymbol{\xi}$ varies when restricted to follow the sparsity pattern \mathbf{l} . in the $p = 3$ example discussed above, $d_{(0,0,0)} = 0$ and $d_{(1,0,0)} = 1$.

Using straightforward calculations, the independent spike-and-slab priors for the off-diagonal entries (specified in (2.2)), can be alternatively represented as a hierarchical prior

distribution as follows:

$$\pi(\boldsymbol{\xi}|\mathbf{l}) = \frac{|\boldsymbol{\Lambda}_{\mathbf{u}}|^{\frac{1}{2}}}{(2\pi)^{\frac{d_{\mathbf{l}}}{2}}} \exp\left(-\frac{\boldsymbol{\xi}'\boldsymbol{\Lambda}\boldsymbol{\xi}}{2}\right) I_{(\boldsymbol{\xi}\in\mathcal{M}_{\mathbf{l}})}, \quad (2.4)$$

where $\boldsymbol{\Lambda}$ is a diagonal matrix with diagonal entries $(\lambda_{jk})_{1\leq j<k\leq p}$, and $\boldsymbol{\Lambda}_{\mathbf{u}}$ is a sub-matrix of $\boldsymbol{\Lambda}$ obtained after removing the rows and columns corresponding to the zeros in $\boldsymbol{\xi}\in\mathcal{M}_{\mathbf{l}}$. In other words, given the sparsity pattern \mathbf{l} , the non-zero entries of $\boldsymbol{\xi}$ follow a $d_{\mathbf{l}}$ -dimensional multivariate normal distribution with mean $\mathbf{0}$ and covariance matrix $\boldsymbol{\Lambda}_{\mathbf{u}}^{-1}$. The marginal distribution of \mathbf{l} is given by

$$\pi(\mathbf{l}) \propto \begin{cases} q^{d_{\mathbf{l}}}(1-q)^{\binom{p}{2}-d_{\mathbf{l}}} & d_{\mathbf{l}} \leq \tau, \\ 0 & d_{\mathbf{l}} > \tau. \end{cases} \quad (2.5)$$

which puts zero mass on *unrealistic sparsity patterns*, i.e., sparsity patterns with more than τ non-zero entries. In the subsequent theoretical analysis, we discuss appropriate values for τ .

Using (2.4) and (2.5), the marginal prior distribution on $\boldsymbol{\xi}$ can be obtained as a mixture of multivariate normal distributions as follows:

$$\pi(\boldsymbol{\xi}) = \sum_{\mathbf{l}\in\mathcal{L}} \pi(\boldsymbol{\xi}|\mathbf{l}) \pi(\mathbf{l}) \propto \sum_{\mathbf{l}\in\mathcal{L}} q^{d_{\mathbf{l}}}(1-q)^{\binom{p}{2}-d_{\mathbf{l}}} \left\{ \frac{|\boldsymbol{\Lambda}_{\mathbf{u}}|^{\frac{1}{2}}}{(2\pi)^{\frac{d_{\mathbf{l}}}{2}}} \exp\left(-\frac{\boldsymbol{\xi}'\boldsymbol{\Lambda}\boldsymbol{\xi}}{2}\right) I_{(\boldsymbol{\xi}\in\mathcal{M}_{\mathbf{l}})} \right\}. \quad (2.6)$$

Note that the vector $\boldsymbol{\xi}$ only incorporates the off-diagonal entries of $\boldsymbol{\Omega}$. Regarding the diagonal entries, we define $\boldsymbol{\delta}$ to be the vector of all diagonal elements $\boldsymbol{\Omega}$, i.e.

$$\boldsymbol{\delta} = (\omega_{11}, \dots, \omega_{pp}). \quad (2.7)$$

Note that an independent $\text{Exponential}(\gamma)$ prior distribution is assigned on each coordinate of $\boldsymbol{\delta}$, i.e.,

$$\pi(\boldsymbol{\delta}) \propto \exp(-\gamma\mathbf{1}'\boldsymbol{\delta}) I_{\mathbb{R}_+^p}(\boldsymbol{\delta}). \quad (2.8)$$

2.1 Computing the Posterior Distribution

Combining (2.1) and (2.2), it is easy to check that the generalized posterior density of $\boldsymbol{\Omega}$ is given by

$$\begin{aligned} \pi\{\boldsymbol{\Omega}|\mathcal{Y}\} \propto & \exp\left(n\sum_{j=1}^p \log\omega_{jj} - \frac{n}{2}\text{tr}(\boldsymbol{\Omega}^2\mathbf{S}) - \lambda\sum_{1\leq j<k\leq p} \frac{\omega_{jk}^2}{2} - \lambda\sum_{j=1}^p \omega_{jj}\right) \\ & \times \prod_{1\leq j<k\leq p} \left(I_{\{0\}}(\omega_{jk}) + \frac{q\sqrt{\lambda_{jk}}}{(1-q)\sqrt{2\pi}} I_{\mathbb{R}\setminus\{0\}}(\omega_{jk})\right). \end{aligned} \quad (2.9)$$

The generalized posterior density in (2.9) is intractable, in the sense that it is not feasible to draw exact samples from such density. However, we will use the conditional posterior density of each element ω_{jk} of $\boldsymbol{\Omega}$, $1\leq j\leq k\leq p$, given the remaining elements denoted by $\boldsymbol{\Omega}_{-(jk)}$, to introduce an entry-wise Gibbs sampler that can generate approximate samples from the

generalized posterior density in (2.9). In order to compute the conditional posterior density of the off-diagonal elements ω_{jk} , $1 \leq j \leq k \leq p$, we first note that

$$n \operatorname{tr}(\boldsymbol{\Omega}^2 \mathbf{S}) = \sum_{i=1}^n \|(\boldsymbol{\Omega} \mathbf{y}_{i\cdot})\|^2 = \sum_{i=1}^n \sum_{j=1}^p \left(\sum_{k=1}^p \omega_{jk} y_{ik} \right)^2 = \sum_{j=1}^p \left\| \left(\sum_{k=1}^p \omega_{jk} \mathbf{y}_{:k} \right) \right\|^2, \quad (2.10)$$

where $\|\cdot\|$ denotes the ℓ_2 norm of a vector.

Thus, in view of (2.10), straightforward algebra shows that

$$\begin{aligned} \pi(\omega_{jk} | \boldsymbol{\Omega}_{-(jk)}, \mathcal{Y}) &\propto \exp \left\{ -\frac{n}{2} (a_{jk} \omega_{jk}^2 + 2b_{jk} \omega_{jk}) \right\} \left(I_{\{0\}}(\omega_{jk}) + \frac{q\sqrt{\lambda}}{(1-q)\sqrt{2\pi}} I_{\mathbb{R} \setminus \{0\}}(\omega_{jk}) \right) \\ &= I_{\{0\}}(\omega_{jk}) + c_{jk} \frac{\sqrt{na_{jk}}}{\sqrt{2\pi}} \exp \left\{ -\frac{na_{jk}}{2} \left(\omega_{jk} + \frac{b_{jk}}{a_{jk}} \right)^2 \right\} I_{\mathbb{R} \setminus \{0\}}(\omega_{jk}) \end{aligned}$$

with,

$$\begin{aligned} a_{jk} &= s_{jj} + s_{kk} + \frac{\lambda_{jk}}{n}, & b_{jk} &= \sum_{k' \neq k} \omega_{jk'} s_{kk'} + \sum_{j' \neq j} \omega_{j'k} s_{jj'} \\ c_{jk} &= \frac{q\sqrt{\lambda_{jk}}}{(1-q)\sqrt{na_{jk}}} \exp \left(\frac{nb_{jk}^2}{2a_{jk}} \right). \end{aligned}$$

Next, letting $p_{jk} = \frac{c_{jk}}{1+c_{jk}}$, we can then write

$$(\omega_{jk} | \boldsymbol{\Omega}_{-(jk)}, \mathcal{Y}) \sim (1 - p_{jk}) I_{\{0\}}(\omega_{jk}) + p_{jk} N\left(-\frac{b_{jk}}{a_{jk}}, \frac{1}{na_{jk}}\right) I_{\mathbb{R} \setminus \{0\}}(\omega_{jk}), \quad 1 \leq j < k \leq p. \quad (2.11)$$

Moreover, the diagonal elements ω_{jj} are conditionally independent and the conditional density of ω_{jj} given $\boldsymbol{\Omega}_{-(jj)}$, $1 \leq j \leq p$, is given by

$$f(\omega_{jj} | \boldsymbol{\Omega}_{-(jj)}, \mathcal{Y}) \propto \omega_{jj}^n \exp \left\{ -\omega_{jj}^2 \left(\frac{n}{2} s_{jj} \right) - \omega_{jj} (\lambda_{jk} + nb_j) \right\}, \quad (2.12)$$

where

$$b_j = \sum_{j' \neq j} \omega'_{jj'} s_{jj'}.$$

Note that the density in 2.12 is not a standard density, but using the fact that it has a unique mode at

$$\frac{-(\lambda_{jk} + nb_j) + \sqrt{(\lambda_{jk} + nb_j)^2 + 4n^2 s_{jj}^k}}{2n s_{jj}^k}, \quad (2.13)$$

one can use a discretization technique to generate samples from it. However, we have observed in our extensive numerical work that the density in (2.12) puts most of its mass around the mode. As a result, when appropriate, one can simply approximate it using a degenerate density with a point mass at its mode, given in 2.13. This approximation allows

faster implementation of the algorithm without sacrificing accuracy. Using the distributions in (2.11) and (2.12), we develop a component-wise Gibbs sampler to generate approximate samples from the joint posterior density in (2.9). Given the current value of Ω , a single iteration of this Gibbs sampler -henceforth referred to as Bayesian Spike and Slab CONCORD (BSSC)- is described in Algorithm 1.

Algorithm 1 Entry wise Gibbs Sampler for BSSC

```

procedure BSSC( $\mathbf{S}$ ) ▷ Input the data
  for  $j = 1, \dots, p - 1$  do
    for  $k = j + 1, \dots, p$  do
       $\omega_{jk} \sim (1 - p_{jk})I_{\{0\}}(\omega_{jk}) + p_{jk}N(-\frac{b_{jk}}{a_{jk}}, \frac{1}{a_{jk}})I_{\mathbb{R} \setminus \{0\}}(\omega_{jk})$ 
    end for
  end for
  for  $j = 1, \dots, p$  do
     $\omega_{jj} \leftarrow \frac{-(\lambda_{jj} + n\Omega'_{-jj}\mathbf{S}_{-jj}) + \sqrt{(\lambda_{jj} + nb_j)^2 + 4n^2s_{ii}^k}}{2ns_{ii}^k}$ 
  end for
  return  $\Omega$  ▷ Return  $\Omega$ 
end procedure

```

Let $\{\hat{\Omega}^{(t)}\}_{t=1}^T$ denote the iterates obtained by running the Gibbs sampler (with a sufficiently long burn-in period). For each $1 \leq j < k \leq p$, we compute the proportion of times the corresponding entry was chosen to be non-zero, i.e.,

$$\hat{p}_{jk} = \frac{1}{T} \sum_{t=1}^T 1_{\{\hat{\omega}_{jk}^{(t)} \neq 0\}}.$$

If \hat{p}_{jk} is greater than a pre-specified threshold $v \in (0, 1)$, (j, k) , the $(j, k)^{th}$ entry is considered to be non-zero in the estimated sparsity pattern for the precision matrix. Note that by the ergodic theorem \hat{p}_{jk} converges to the posterior probability of ω_{jk} being non-zero as $T \rightarrow 0$. Hence, an entry is classified as non-zero, if the posterior probability of being non-zero is above v . We denote the resulting sparsity pattern estimate by $\hat{\mathbf{I}}_{v, BSSC}$, and use the threshold $v = 0.5$ in our numerical work to obtain the *median probability model/sparsity pattern*. The user has the flexibility to select more conservative or relaxed threshold values.

Remark 1. (*Selection of hyperparameters*) A good selection of shrinkage hyperparameters $\{\lambda_{jk}\}_{1 \leq j < k \leq p}$ and $\{\gamma_j\}_{j=1}^p$, along with the mixing probability q is important. Following Park and Casella [2008], Wang et al. [2012], independent gamma prior distributions are assigned on each shrinkage parameter λ_{jk} and γ_j , i.e.,

$$\lambda_{jk} \sim \text{Gamma}(r, s) \quad \text{for } 1 \leq j < k \leq p, \quad \gamma_j \sim \text{Gamma}(r, s) \quad \text{for } 1 \leq j \leq p$$

for some fixed $r, s > 0$. Straightforward calculations demonstrate that $\{\lambda_{jk}\}_{1 \leq j < k \leq p}, \{\gamma_j\}_{j=1}^p$ are conditionally mutually independent given Ω, \mathcal{Y} , i.e.,

$$\lambda_{jk} \mid \Omega, \mathcal{Y} \sim \text{Gamma}(r + 0.5, 0.5\omega_{jk}^2 + s), \quad \gamma_j \mid \Omega, \mathcal{Y} \sim \text{Gamma}(r + 1, \omega_{jj} + s).$$

Since $\mathbb{E}\{\lambda_{jk} \mid \Omega, \mathcal{Y}\} = \frac{r+0.5}{0.5\omega_{jk}^2+s}$ and $\mathbb{E}\{\gamma_j \mid \Omega, \mathcal{Y}\} = \frac{r+1}{\omega_{jj}+s}$, this approach selects the respective shrinkage parameters based on the current ω -values in a way that larger (smaller) entries are regularized less (more) on average. For the parameters r and s of the Gamma prior distribution, in absence of any prior information, we recommend the non-informative choices $r = 10^{-4}$ and $s = 10^{-8}$, which come very close to flat prior distributions for the λ and γ values, and are based on the suggestions made in Wang et al. [2012]. Extensive numerical work suggests (see Section 4) that these are satisfactory choices.

The default choice for the mixing probability q is the objective one, namely $q = 1/2$. Based on the consistency results in Section 3, one can use the choice $q = 1/p$ in really high-dimensional settings to further encourage sparser models.

2.2 Estimating magnitudes of non-zero entries: Correcting for bias using refitting

As previously mentioned, the key objective of the B-CONCORD methodology is the identification of the correct sparsity pattern in the precision matrix Ω . However, a good estimate of the “strength” (magnitude) of the conditional association between two variables is also required for downstream analysis in many applications. Note that such estimates can be obtained from Algorithm 1, and Theorem 2 establishes their asymptotic accuracy and convergence rates under high-dimensional scaling. Nevertheless, in finite sample settings these estimates exhibit bias, an issue also noticed in the frequentist literature and resolved through the development of debiasing procedures Zhang and Zhang [2014], Javanmard and Montanari [2014], Van De Geer [2019]). The numerical work in Section 4 also provides evidence for the presence of bias.

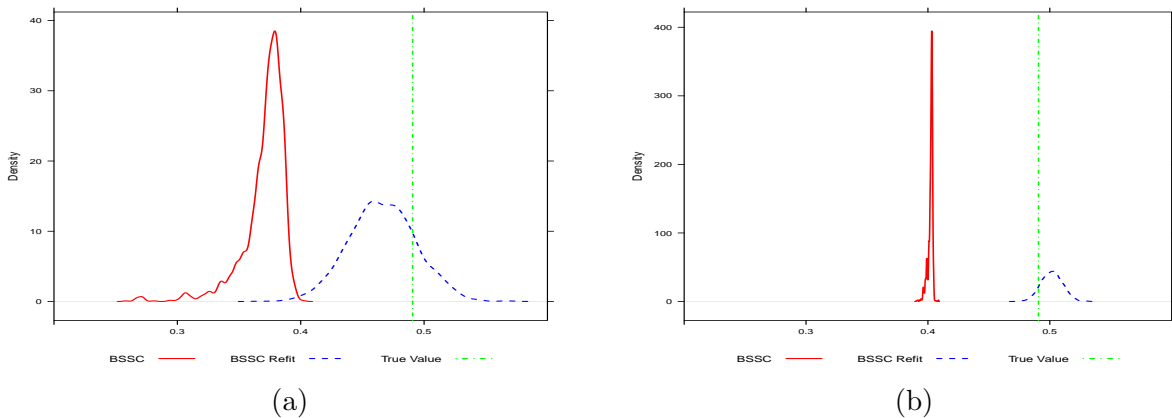
A popular approach for addressing this problem for regularized estimates in a frequentist setting is to employ a refitting step, wherein only the non-zero entries of the precision matrix are re-estimated (e.g., see Ma and Michailidis [2016]). Next, we propose a Bayesian refitting step for obtaining debiased/improved estimates of the magnitudes of the non-zero entries of Ω (as specified by the sparsity pattern obtained from Algorithm 1). Figure 1 is an illustration of the effectiveness of the refitting technique, described later in this section. The plot depicts the estimation accuracy for one coefficient of a precision matrix of dimension $p = 50$ based on sample sizes $n = 100$ (panel 1a) and $n = 1000$ (panel 1b). The posterior density of the coefficient was estimated using both BSSC and the refitting approach, colored in red and blue, respectively. The true coefficient value corresponds to the green vertical line. Figure 1 shows that the true coefficient is located within the range of the estimated posterior density generated by the refitting approach. Theorem 2 theoretically establishes posterior estimation consistency of the refitting approach. In addition, in section 4.2, we further demonstrate the numerical significance of the refitting approach in reducing the estimation error.

Recall from the discussion at the end of Section 2.1 that using the output of Algorithm 1, the proportion of times the $(j, k)^{th}$ entry was non-zero in the iterates of the sampler (denoted by \hat{p}_{jk}) can be computed. Let v be the user specified threshold, and let

$$\hat{E} = \{(j, k) : \hat{p}_{jk} > v\} \tag{2.14}$$

denote the collection of indices classified as non-zero. Let \hat{G} denote the graph with vertices

Figure 1: Illustrating the presence of bias in the output of Algorithm 1) and its correction through a refitting step for a coefficient from a $p = 50$ dimensional precision matrix, estimated from $n = 100$ (panel (a)) and $n = 1000$ (panel (b)) samples.



$\{1, 2, \dots, p\}$ and edge set \hat{E} . In other words, \hat{G} encodes the sparsity pattern of $\hat{\Omega}$. Let $\mathbb{M}_{\hat{G}}$ be defined as

$$\mathbb{M}_{\hat{G}} = \left\{ \Omega \in \mathbb{M}_p^+ : M_{ij} = 0 \text{ if } i \neq j, (i, j) \notin \hat{E} \right\},$$

which is the space of symmetric $p \times p$ matrices with positive diagonal entries obeying the sparsity pattern encoded in \hat{G} . The goal is to construct a debiased/improved estimate (and corresponding credible region) for $\Omega \in \mathbb{M}_{\hat{G}}$ by specifying an appropriate prior distribution on $\mathbb{M}_{\hat{G}}$.

An immediate question that might arise in the mind of the reader is that while the positive definite constraint can be relaxed for the purpose of estimating the sparsity pattern in Ω , this constraint should be imposed for estimating the magnitudes of the entries of Ω . One can certainly do this by further restricting to the space $\mathbb{P}_{\hat{G}}$ (which is defined to be the intersection of $\mathbb{M}_{\hat{G}}$ with positive definite matrices), specifying a prior on $\mathbb{P}_{\hat{G}}$, and then using the subsequent posterior distribution. This however leads to significant computational challenges and involves inversion of $p - 1$ dimensional matrices. Hence, for computational reasons, we first construct our prior on $\mathbb{M}_{\hat{G}}$, and project the resulting estimator (and associated credible region) on the space of positive definite matrices by modifying the diagonal entries (see the end of this section for details).

We start by specifying an improper prior distribution on $\mathbb{M}_{\hat{G}}$, and explain why we expect the resulting posterior distribution to lead to good estimators. We specify independent (improper) uniform priors on the off-diagonal entries $\{\omega_{jk}\}_{(j,k) \in E}$ and for the diagonal entries we independently specify the following improper priors:

$$\pi(\omega_{jj}) \propto \exp(n\omega_{jj} - n \log \omega_{jj}), \quad \omega_{jj} > 0, \quad \text{for } 1 \leq j \leq p. \quad (2.15)$$

Then, the joint posterior distribution on $\mathbb{M}_{\hat{G}}$ is given by

$$\pi_{\text{refitted}}(\Omega | \mathcal{Y}) \propto \exp\left\{n \text{tr}(\Omega) - \frac{n}{2} \text{tr}(\Omega^2 \mathbf{S})\right\} \text{ for } \Omega \in \mathbb{M}_{\hat{G}}. \quad (2.16)$$

We refer to this posterior distribution as the **refitted posterior**, since it is defined conditional on the sparsity pattern estimated from Algorithm 1 and encoded in \hat{G} . The following lemma addresses the propriety and unimodality of the posterior distribution, and its proof can be found in the Supplement.

Lemma 1. *If the degree of \hat{G} (maximum number of edges shared by any vertex) is less than n , then the following holds.*

1. *The refitted posterior density in (2.16) can be normalized to a proper probability density.*
2. *This refitted posterior density is log-concave and has a unique mode.*

The next lemma provides insights on why the mode of the refitted posterior distribution is a good/improved estimator of Ω .

Lemma 2. *Suppose $\mathbf{K} \in \mathbb{P}_{\hat{G}}$. Then,*

$$\mathbf{K} = \arg \min_{\Omega \in \mathbb{M}_{\hat{G}}} \left\{ \frac{n}{2} \text{tr}(\Omega^2 \mathbf{K}^{-1}) - n \text{tr}(\Omega) \right\}.$$

Suppose the true precision matrix $\Omega^0 = (\Sigma^0)^{-1}$ belongs to \mathbb{M}_G for some graph G . Then, it follows from Lemma 2 that

$$\Omega^0 = \arg \min_{\Omega \in \mathbb{M}_G} \left\{ \frac{n}{2} \text{tr}(\Omega^2 \Sigma^0) - n \text{tr}(\Omega) \right\}.$$

Note that under mild regularity assumptions, the maximum entry-wise difference between the sample covariance matrix and the population covariance matrix is of the order $\sqrt{\log p/n}$. Hence, if \hat{G} (obtained from Algorithm 1) is an accurate estimate of the true underlying graph G for the true precision matrix Ω^0 , we expect that the mode of the refitted posterior density in (2.16), given by

$$\hat{\Omega}_{\text{mode, refitted}} = \arg \min_{\Omega \in \mathbb{M}_{\hat{G}}} \left\{ \frac{n}{2} \text{tr}(\Omega^2 S) - n \text{tr}(\Omega) \right\},$$

is close to Ω^0 . This heuristic analysis is formalized in a high-dimensional setting in Theorem 2.

It follows from Lemma 1 that the mode of the refitted posterior density is available in closed form. To compute credible intervals, we observe that the full conditional posterior densities of the non-zero elements in $\mathbb{M}_{\hat{G}}$ can be derived in a straightforward way. Let \hat{E} denote the edge set for \hat{G} . In particular, it can be shown that the full conditional (refitted) posterior density of ω_{jk} for $(j, k) \in \hat{E}$ is

$$N \left(-\frac{b_{jk}}{a_{jk}}, \frac{1}{na_{jk}} \right) \tag{2.17}$$

where

$$a_{jk} = s_{jj} + s_{kk}, \quad b_{jk} = \sum_{k' \neq k, (j, k') \in E} \omega'_{jk'} s_{kk'} + \sum_{j' \neq j, (j', k) \in E} \omega_{j'k} s_{jj'}.$$

Further, the full conditional (refitted) posterior density of ω_{jj} is

$$\text{trunc}N\left(\frac{1-b_j}{s_{jj}}, \frac{1}{ns_{jj}}, 0, \infty\right), \quad (2.18)$$

where

$$b_j = \sum_{j' \neq j, (j, j') \in E} \omega'_{jj'} s_{jj'}$$

and $\text{trunc}N(\mu, \sigma^2, u, v)$ denotes a normal distribution with mean μ and variance σ^2 , truncated in the interval (u, v) . Hence, one can generate approximate samples from the refitted posterior density using a Gibbs sampling approach. These samples can be subsequently used to generate a posterior credible region.

As previously discussed, the refitted posterior density is supported on $\mathbb{M}_{\hat{G}}$, and hence the mode/mean is not guaranteed to be positive definite. However, our numerical work shows that as long as the sample size is not too small -e.g., $n > p/2$ -, the resulting estimated precision matrix will actually be positive definite.

In case the sample size was really small, the resulting estimated precision matrix may not be positive definite. In such circumstances, a crude but simple solution, if needed, is to “project” the posterior mode/mean (and the associated credible region) on the space of positive definite matrices by using the following transformation

$$B(\Omega) = \begin{cases} \Omega & \text{if } \Omega \text{ is positive definite,} \\ \Omega - \lambda_{\min}(\Omega)I_p + \epsilon I_p & \text{if } \lambda_{\min}(\Omega) \leq 0, \end{cases}$$

where $\epsilon > 0$ is a user-defined small positive number. The function B leaves positive definite matrices in $\mathcal{M}_{\hat{G}}$ invariant, and appropriately increases the diagonal entries of matrices that are not positive definite.

As previously mentioned, the main goal of this paper is selecting the sparsity pattern in Ω . The refitting and projection based method developed in this section for estimating the magnitude of the non-zero entries (post sparsity selection) performs well in the simulations in Section 4, and indeed reduces bias. Developing more sophisticated, and yet computationally effective methods for projecting into the space of (sparse) positive definite matrices is a topic of current research.

3 High Dimensional Sparsity Selection Consistency and Convergence Rates for B-CONCORD

In this section, we establish selection and estimation consistency properties for B-CONCORD, under high dimensional scaling wherein the number of variables $p = p_n$ increases with the sample size n . The observations $\mathbf{y}_1^n, \mathbf{y}_2^n, \dots, \mathbf{y}_n^n \in \mathbb{R}^{p_n}$ form an i.i.d. sample from a distribution with mean $\mathbf{0}$ and precision matrix Ω_n^0 . Let $G_n^0 = (\{1, 2, \dots, p_n\}, E_{0,n})$ denote the graph encoding the sparsity pattern in Ω_n^0 . Let $\mathbf{t} = \mathbf{t}_n \in \{0, 1\}^{\binom{p}{2}}$ denote the sparsity pattern in the true precision matrix Ω_n^0 , and $d_{\mathbf{t},n}$ denote the number of non-zero entries in \mathbf{t} . For ease

of exposition, we will often suppress the dependence of the quantities $p_n, \boldsymbol{\Omega}_n^0, G_n^0, \mathbf{t}_n, d_{t,n}$ on n , and simply denote them by $p, \boldsymbol{\Omega}^0, G^0, \mathbf{t}, d_t$, respectively.

Recall from (2.3) and (2.7) that $\boldsymbol{\xi}$ and $\boldsymbol{\delta}$ denote the vectorized versions of the off-diagonal and diagonal entries of $\boldsymbol{\Omega}$. Let $\boldsymbol{\xi}^0$ denote the vectorized version of the off-diagonal elements of the true precision matrix $\boldsymbol{\Omega}^0$. Using (2.6), (2.8), (2.9), and straightforward calculations, the generalized posterior distribution in terms of the $(\boldsymbol{\xi}, \boldsymbol{\delta})$ can be expressed as

$$\begin{aligned} \pi \{ \boldsymbol{\xi}, \boldsymbol{\delta} \mid \mathcal{Y} \} &\propto \exp \left\{ n \mathbf{1}' \log(\boldsymbol{\delta}) - \frac{n}{2} \left[\begin{pmatrix} \boldsymbol{\xi}' & \boldsymbol{\delta}' \end{pmatrix} \begin{pmatrix} \boldsymbol{\Phi} & \mathbf{A} \\ \mathbf{A}' & \mathbf{D} \end{pmatrix} \begin{pmatrix} \boldsymbol{\xi} \\ \boldsymbol{\delta} \end{pmatrix} \right] \right\} \exp \left(-\frac{\boldsymbol{\xi}' \boldsymbol{\Lambda} \boldsymbol{\xi}}{2} \right) \\ &\quad \times \sum_{\mathbf{l} \in \mathcal{L}} \left\{ \frac{|\boldsymbol{\Lambda} \mathbf{u}|^{\frac{1}{2}}}{(2\pi)^{\frac{d_{\mathbf{l}}}{2}}} I_{(\boldsymbol{\xi} \in \mathcal{M}_{\mathbf{l}})} \left[q^{d_{\mathbf{l}}} (1-q)^{\binom{p}{2} - d_{\mathbf{l}}} \right] \right\} \exp(-\gamma \mathbf{1}' \boldsymbol{\delta}). \end{aligned} \quad (3.1)$$

where, $\boldsymbol{\Phi}$ is a $\frac{p(p-1)}{2} \times \frac{p(p-1)}{2}$ symmetric matrix which after indexing the rows and columns using $(12, 13, \dots, p-1p)$, is given by

$$\boldsymbol{\Phi}_{(ab,cd)} = \begin{cases} s_{aa} + s_{bb} & \text{if } a = b \ \& \ c = d, \\ s_{ac} & \text{if } b = d \ \& \ a \neq c, \\ s_{bd} & \text{if } a = c \ \& \ b \neq d, \\ 0 & \text{if } a \neq b \ \& \ c \neq d, \end{cases} \quad \text{for } 1 \leq a < b \leq p, \text{ and } 1 \leq c < d \leq p. \quad (3.2)$$

For example, when $p = 5$, $\boldsymbol{\Phi}$ is as follows.

$$\begin{pmatrix} s_{11} + s_{22} & s_{23} & s_{24} & s_{25} & s_{13} & s_{14} & s_{15} & 0 & 0 & 0 \\ s_{23} & s_{11} + s_{33} & s_{34} & s_{35} & s_{12} & 0 & 0 & s_{14} & s_{15} & 0 \\ s_{24} & s_{34} & s_{11} + s_{44} & s_{45} & 0 & s_{12} & 0 & s_{13} & 0 & s_{15} \\ s_{25} & s_{35} & s_{45} & s_{11} + s_{55} & 0 & 0 & s_{12} & 0 & s_{13} & s_{14} \\ s_{13} & s_{12} & 0 & 0 & s_{22} + s_{33} & s_{34} & s_{35} & s_{24} & s_{25} & 0 \\ s_{14} & 0 & s_{12} & 0 & s_{34} & s_{22} + s_{44} & s_{45} & s_{23} & 0 & s_{25} \\ s_{15} & 0 & 0 & s_{12} & s_{35} & s_{45} & s_{22} + s_{55} & 0 & s_{23} & s_{24} \\ 0 & s_{14} & s_{13} & 0 & s_{24} & s_{23} & 0 & s_{33} + s_{44} & s_{45} & s_{35} \\ 0 & s_{15} & 0 & s_{13} & s_{25} & 0 & s_{23} & s_{45} & s_{33} + s_{55} & s_{34} \\ 0 & 0 & s_{15} & s_{14} & 0 & s_{25} & s_{24} & s_{35} & s_{34} & s_{44} + s_{55} \end{pmatrix},$$

In addition, the vector \mathbf{a} is a vector of length $\frac{p(p-1)}{2}$ given by

$$\mathbf{a} = (s_{12}(\omega_{11} + \omega_{22}), \dots, s_{1p}(\omega_{11} + \omega_{pp}), \dots, s_{p-1p}(\omega_{p-1p-1} + \omega_{pp}))', \quad (3.3)$$

\mathbf{A} is a $\frac{p(p-1)}{2} \times p$ matrix such that $\mathbf{A}\boldsymbol{\delta} = \mathbf{a}$ and \mathbf{D} is a $p \times p$ diagonal matrix with entries $\{s_{ii}\}_{1 \leq i \leq p}$. Recall that \mathcal{L} denotes the space of all the $2^{\binom{p}{2}}$ sparsity patterns for $\boldsymbol{\xi}$, and $\mathcal{M}_{\mathbf{l}}$ denotes the space in which the parameter $\boldsymbol{\xi}$ varies when restricted to the sparsity pattern \mathbf{l} .

Note that our main objective is to correctly select that sparsity pattern in the off-diagonal entries. Hence, as commonly done for generalized likelihood based high-dimensional consistency proofs - see Khare et al. [2015], Peng et al. [2009] - we assume the existence of accurate estimates for the diagonal elements, i.e., estimates $\hat{\omega}_{ii}$ are available, such that for any $\eta > 0$, there exists a constant $C > 0$, such that

$$\max_{1 \leq k \leq K} \|\hat{\omega}_{ii} - \omega_{ii}\| \leq C \left(\sqrt{\frac{\log p}{n}} \right), \quad (3.4)$$

with probability at least $1 - O(n^{-\eta})$. One way to get such estimates of the diagonal entries is discussed in Lemma 4 of Khare et al. [2015]. Denote the resulting estimates of the vectors $\boldsymbol{\delta}$ and \boldsymbol{a} by $\hat{\boldsymbol{\delta}}$ and $\hat{\boldsymbol{a}}$, respectively. For the remainder of the section, we assume that the entries of $\boldsymbol{\Lambda}$ are fixed.

In view of (3.1), the conditional posterior distribution of the vector of off-diagonal entries $\boldsymbol{\xi}$ given $\hat{\boldsymbol{\delta}}$ is as follows.

$$\begin{aligned} \pi \left\{ \boldsymbol{\xi} | \hat{\boldsymbol{\delta}}, \mathcal{Y} \right\} &\propto \exp \left\{ -\frac{1}{2} [\boldsymbol{\xi}' (n\boldsymbol{\Phi} + \boldsymbol{\Lambda}) \boldsymbol{\xi} + 2n\boldsymbol{\xi}' \hat{\boldsymbol{a}}] \right\} \\ &\times \sum_{\ell \in \mathcal{L}} \left\{ \frac{|\boldsymbol{\Lambda}_{\ell\ell}|^{\frac{1}{2}}}{(2\pi)^{\frac{d_\ell}{2}}} I_{(\boldsymbol{\xi} \in \mathcal{M}_\ell)} \left[q^{d_\ell} (1-q)^{\binom{p}{2} - d_\ell} \right] \right\}, \end{aligned} \quad (3.5)$$

The above posterior distribution is a mixture distribution, and induces a posterior distribution on the space of sparsity patterns. Straightforward calculations (see proof of Lemma S4 in the Supplemental document) show that

$$\pi \left\{ \ell | \hat{\boldsymbol{\delta}}, \mathcal{Y} \right\} \propto q^{d_\ell} (1-q)^{\binom{p}{2} - d_\ell} \frac{|\boldsymbol{\Lambda}_{\ell\ell}|^{\frac{1}{2}}}{|(n\boldsymbol{\Phi} + \boldsymbol{\Lambda})_{\ell\ell}|^{\frac{1}{2}}} \exp \left\{ \frac{n^2}{2} \hat{\boldsymbol{a}}_\ell' (n\boldsymbol{\Phi} + \boldsymbol{\Lambda})_{\ell\ell}^{-1} \hat{\boldsymbol{a}}_\ell \right\}. \quad (3.6)$$

for every $\ell \in \mathcal{L}$. To establish high-dimensional asymptotic properties of this posterior distribution on the space of sparsity patterns, the following standard and mild regularity assumptions are made.

Assumption 1. $(d_t + 1) \sqrt{\frac{\log p}{n}} \rightarrow 0$, as $n \rightarrow \infty$.

This assumption essentially states that the number of variables p has to grow slower than $e^{\binom{n}{d_t}}$. Similar assumptions have been made in other high dimensional covariance estimation methods e.g. Banerjee and Ghosal [2014], Banerjee and Ghosal [2015], Bickel and Levina [2008], and Xiang et al. [2015].

Assumption 2. *There exists $c > 0$, independent of n such that*

$$\mathbb{E}_0 [\exp(\boldsymbol{\alpha}' \mathbf{y}_i)] \leq \exp(c\boldsymbol{\alpha}' \boldsymbol{\alpha}),$$

where \mathbb{E}_0 denotes the expected value with respect to the true data generating model. The above assumption allows for deviations from normality. Hence, Theorem 1 below establishes that B-CONCORD is robust (in terms of consistency) under misspecification of the data generating distribution, as long as its tails are sub-Gaussian.

Assumption 3. *(Bounded eigenvalues). There exists $\tilde{\varepsilon}_0 > 0$, independent of n , such that*

$$\tilde{\varepsilon}_0 \leq \text{eig}_{\min}(\boldsymbol{\Omega}^0) \leq \text{eig}_{\max}(\boldsymbol{\Omega}^0) \leq \frac{1}{\tilde{\varepsilon}_0}.$$

This is a standard assumption in high dimensional analysis to obtain consistency results; see for example Bühlmann and Van De Geer [2011].

Assumption 4. (*Signal Strength*). Let s_n be the smallest non-zero entry (in magnitude) in the vector $\boldsymbol{\xi}_0$. We assume $\frac{\frac{1}{2} \log n + d_t \log p}{ns_n^2} \rightarrow 0$.

This is again a standard assumption. Similar assumptions on the appropriate signal size can be found in Khare et al. [2015], Peng et al. [2009].

Assumption 5. (*Decay rate of the edge probabilities*). Let $q = p^{-a_2 d_t}$, where $a_2 = \frac{16 \max(1, c_0)^2}{\min(1, \bar{\varepsilon}_0)}$.

Here c_0 is a constant (not depending in n) that is specified in the proof of Lemma S 3 in the Supplemental Document. This assumption can be interpreted as a priori penalizing sparsity patterns with too many non-zero entries. Next, we establish the main posterior consistency result. In particular, we show that the posterior mass assigned to the true sparsity pattern converges to one in probability (under the true model), if we restrict to *realistic sparsity patterns*, i.e., sparsity patterns where the number of non-zero entries is bounded by τ_n , an appropriate constant multiple of $\sqrt{\frac{n}{\log p}}$ (see Lemma S 2 in the Supplemental Document).

Theorem 1. (*Strong Selection Consistency*) Under Assumptions 1 - 5, and restricting to realistic sparsity patterns, the posterior distribution on the sparsity patterns in (3.6) puts all of its mass on the true sparsity pattern \mathbf{t} as $n \rightarrow \infty$, i.e.,

1.
$$\pi \left\{ \mathbf{t} | \hat{\boldsymbol{\delta}}, \mathcal{Y} \right\} \xrightarrow{\mathbb{P}_0} 1, \quad \text{as } n \rightarrow \infty. \quad (3.7)$$

2. The sparsity pattern estimate $\hat{\mathbf{l}}_{v, BSSC}$, obtained by using the output of the BSSC Algorithm and applying the thresholding approach discussed at the end of Section 2.1, satisfies

$$\mathbb{P}_0 \left(\hat{\mathbf{l}}_{v, BSSC} = \mathbf{t} \right) \rightarrow 1 \quad \text{as } n \rightarrow \infty.$$

While the main objective is sparsity selection consistency, we also derive a result that establish estimation consistency/ convergence rates for the estimates of the magnitudes of the non-zero entries obtained from the refitted posterior density defined in (2.16).

For every $1 \leq i \leq p$, let ν_i^0 denote the number of structurally non-zero off-diagonal entries in the i^{th} row (or column) of $\boldsymbol{\Omega}^0$. It follows that $d_t = \frac{1}{2} \sum_{i=1}^p \nu_i^0$. Let

$$\nu_{\max} = \max_{1 \leq i \leq p} \nu_i^0$$

denote the maximum number of non-zero entries in any row (or column) of $\boldsymbol{\Omega}^0$. The relationship between ν_{\max} and d_t (total number of structurally non-zero entries in $\boldsymbol{\Omega}^0$) depends on the underlying sparsity structure. At one extreme, ν_{\max} can be the same order as d_t (eg. star graph), while at the other extreme it can be as small as $O(d_t/p)$ (eg. banded matrix). For the posterior convergence rate result, we use the same assumptions as Theorem 1, except Assumption 1, which is replaced by the slightly stronger assumption below.

Assumption 6. $(d_t + \sqrt{d_t} \nu_{\max} + 1) \sqrt{\frac{\log p}{n}} \rightarrow 0$, as $n \rightarrow \infty$.

In many settings, where $\nu_{\max} = O(\sqrt{d_t})$, Assumption 1 and Assumption 6 are equivalent.

Theorem 2. (*Estimation Consistency and convergence rate for refitted posterior*) Under Assumptions 2 - 6, the refitted posterior density $\pi_{refitted}$ in (2.16) satisfies

$$\mathbb{E}_0 \left[\pi_{refitted} \left(\left\| \hat{\Omega} - \Omega^0 \right\|_{\max} > K \nu_{\max} \sqrt{\frac{d_t \log p}{n}} \right) \right] \rightarrow 0 \quad \text{as } n \rightarrow \infty,$$

for a large enough constant K (not depending on n), and

$$\mathbb{E}_0 \left[\pi_{refitted} \left(\left\| \hat{\Omega} - \Omega^0 \right\| > K \nu_{\max}^2 \sqrt{\frac{d_t \log p}{n}} \right) \right] \rightarrow 0 \quad \text{as } n \rightarrow \infty.$$

Here $\| \cdot \|_{\max}$ denotes the sup norm of a matrix (magnitude of entry with largest absolute value), and $\| \cdot \|$ denotes the operator norm of a matrix. The proofs of the two results above are provided in the Section S3 of the Supplement.

Remark 2. *Posterior estimation consistency/contraction rates for some pseudo-likelihood based Bayesian approaches have been studied in recent work by Atchadé et al. [2017]. In particular, a **discrete binary** graphical model (as opposed to a partial correlation network for continuous variables in this study) is one of the models considered in Atchadé et al. [2017]. A posterior contraction rate of $\sqrt{\frac{(p+d_t) \log p}{n}}$ for Ω in the Frobenius norm is obtained without making an assumption similar to our assumption of accurate diagonal estimates. Note however that results in Atchadé et al. [2017] do not address model selection consistency.*

4 Performance Evaluation of B-CONCORD

We assess the accuracy, computational speed and scalability of the BSSC Algorithm. As mentioned earlier, the main challenge with existing Bayesian procedures is their limited scalability. To the best of our knowledge, Stochastic Search Structure Learning (SSSL) introduced in Wang [2015] is the fastest Bayesian procedure available for the problem at hand (see Section 5 of Wang [2015]). Hence, we use SSSL as a benchmark for the performance of our BSSC Algorithm.

4.1 Computational scalability: Timing and memory requirement comparison

For this task, we set $p \in \{150, 300, 500, 1000, 3000\}$. For each p , the *true* precision matrix Ω^0 is generated so as to exhibit a complete random sparsity patterns with 4% density of non-zero entries. The non-zero off-diagonal entries are generated from a Uniform distribution in the interval $[-0.6, -0.4] \cup [0.4, 0.6]$, and the diagonal entries are adjusted as needed to make the resulting precision matrix positive definite. We then generate 25 data sets of size $n = p/2$ from a multivariate Gaussian distribution with mean $\mathbf{0}$ and precision matrix Ω^0 . The BSSC Algorithm (with default hyperparameter values as discussed in Remark 1), the SSSL procedure (with default hyperparameter values as specified in Wang [2015] and

graphical lasso (Glasso) (with the final value of its shrinkage parameter manually selected using exhaustive cross-validations) are used to obtain estimates of Ω^0 .

For the BSSC Algorithm 1, 2000 iterations are used for burn-in, and 2000 more iterations to generate our estimates (standard diagnostics indicate that so many iterations are sufficient for convergence). For SSSL and with $p \in \{150, 300\}$, we used the default setting in Wang [2015] of 1000 iterations for burn-in, and 10000 iterations for computing posterior estimates; however, for higher dimensions -e.g. $p \in \{500, 1000, 3000\}$ - the default setting required more than 50 GigaBytes of memory and therefore only 500 iterations for burn-in and 500 iterations for computing posterior estimates were used. Finally, the results for Glasso were achieved using the default number of iterations for convergence. The two Bayesian algorithms are compared based on *computing time required per iteration*. The simulations were performed using dedicated cores at the High Performance Computing cluster at the University of Florida.

Table 1 depicts *computing time required per iteration* for BSSC, SSSL, and Glasso averaged over the 25 replicate data sets. The results demonstrate that SSSL becomes expensive even for $p = 500$, while BSSC easily handles settings with $p \geq 1000$. Each BSSC iterate requires less than 44 seconds, which is a fraction ($1/5760$) of an SSSL iterate. Further, each BSSC iterate is faster than a Glasso one, thus making the two procedures comparable in total computational time required for estimating precision matrices with $p \leq 300$. However, Glasso has an overall time execution advantage for larger p , since it requires on average less than 10 iterations to converge and provide estimates.

Table 1: Average wall-clock seconds per iteration for BSSC, Glasso, and SSSL for estimating a $p \times p$ precision matrix with $p \in (150, 300, 500, 1000$ and $3000)$.

	$p = 150$	$p = 300$	$p = 500$	$p = 1000$	$p = 3000$
BSC	0.006	0.035	0.112	0.675	43.122
Glasso	0.108	0.293	0.523	5.857	168.333
SSSL	0.104	1.31	10.1	37.38	237600

In addition, the memory requirement for BSSC is significantly smaller than SSSL. The average memory used by BSSC and SSSL for different values of p is summarized in Table 2. Note that SSSL requires more than 50 GB for $p \geq 500$ while BSSC achieves the goal with 0.24 GB of memory.

Table 2: Average memory usage (in GigaBytes) for BSSC and SSSL for estimating a $p \times p$ precision matrix with $p \in (150, 300, 500, 1000$ and $3000)$.

	$p = 150$	$p = 300$	$p = 500$	$p = 1000$	$p = 3000$
BSC	0.001	0.22	0.24	0.32	1.39
SSSL	5.3	20.4	>50	>50	>50

The reason for the significantly superior performance of BSSC compared to SSSL is discussed next. The SSSL algorithm requires $2(p - 1)$ matrix inversions of $(p - 1) \times (p - 1)$ matrices (see Section 4.1 of Wang [2015]). The worst case computational complexity for one iteration

of the SSSL algorithm therefore is $O(p^4)$. On the other hand, one iteration of the BSSC algorithm has computational complexity $O(p^3)$ (update each of the $\binom{p}{2}$ entries with $O(p)$ computations, see Algorithm 1), and requires *no matrix inversions*. For sparse precision matrices, computational complexity in practice is better for both methods than the above worse case scenarios. Nevertheless, the numerical results presented amply demonstrate the superior performance of BSSC. Note that in sparse settings, it becomes faster to compute inner products of the form $\boldsymbol{\Omega}'_{-jk}\mathbf{S}_{-jj}$ needed by BSSC.

4.2 Estimation accuracy comparison

The standard performance metrics of specificity (SP), sensitivity (SE) and Matthews Correlation Coefficient (MCC), defined next, are used.

$$\begin{aligned} \text{SP} &= \frac{\text{TN}}{\text{TN} + \text{FP}}, & \text{SE} &= \frac{\text{TP}}{\text{TP} + \text{FN}} \\ \text{MCC} &= \frac{\text{TP} \times \text{TN} - \text{FP} \times \text{FN}}{\sqrt{(\text{TP} + \text{FP})(\text{TP} + \text{FN})(\text{TN} + \text{FP})(\text{TN} + \text{FN})}} \end{aligned} \quad (4.1)$$

where TP, TN, FP and FN represent the number of true positives, true negatives, false positives and false negatives, respectively. Larger values of any of the above metrics indicate better sparsity selection obtained by the corresponding algorithm. Precision matrices of dimension $p \in (150, 300, 500, \text{ and } 1000)$, and sample size $n \in (p/2, 3p/4, p, \text{ and } 2p)$ are considered. Further, the proportion of non-zero upper off-diagonal entries of $\boldsymbol{\Omega}^0$ is set to 0.04 and 0.1. The true precision matrix is generated according to the same mechanism as in Section 4.1. For each combination of p , n , and edge density level, we generate 50 data sets of size n from a multivariate normal distribution with mean $\mathbf{0}$ and precision matrix $\boldsymbol{\Omega}^0$. For each data set, we estimate the sparsity pattern using BSSC and SSSL, and subsequently calculate the SP, SE, MCC measures. The same number of burn-in (2000) and estimation (2000) iterations are used for BSSC. For small $p \in \{150, 300\}$, we used the default setting in Wang [2015] of 1000 iterations for burn-in, and 10000 iterations for computing posterior estimates. For the reasons previously discussed, we only used 500 iterations for burn-in and 500 iterations for estimation purposes for $p = 500, 1000$.

The SP, SE, MCC values, averaged over 50 replicate data sets, are provided in Table 3. Overall, the MCC values indicate better sparsity selection achieved by BSSC compared to SSSL, when the density of non-zeros entries is 0.1, while the results are comparable for 0.04 density. In summary, BSSC outperforms SSSL both in terms of estimation accuracy and especially of computational requirements on execution time and memory.

Table 3: Average sparsity selection accuracy for BSSC and SSSL for estimating a $p \times p$ precision matrix with $p \in (150, 300, 500, \text{ and } 1000)$.

		BSSC				SSSL			
		$p = 150$	$p = 300$	$p = 500$	$p = 1000$	$p = 150$	$p = 300$	$p = 500$	$p = 1000$
n		<i>Density = 0.04</i>				<i>Density = 0.04</i>			
$p/2$	SP%	99	100	100	100	100	100	100	100
	SE%	26	28	29	30	20	22	17	17
	MC%	41	44	45	46	39	42	37	36
$3p/4$	SP%	99	100	100	100	100	100	100	100
	SE%	41	43	45	47	34	35	29	28
	MC%	55	58	60	62	54	56	50	49
p	SP%	100	100	100	100	100	100	100	100
	SE%	53	57	60	61	45	48	41	38
	MC%	67	70	71	73	64	67	61	58
$2p$	SP%	100	100	100	100	100	100	100	100
	SE%	86	89	91	92	78	85	79	74
	MC%	89	91	92	93	87	91	88	85
n		<i>Density = 0.1</i>				<i>Density = 0.1</i>			
$p/2$	SP%	99	99	99	99	100	100	100	100
	SE%	12	11	10	11	9	4	6	5
	MC%	24	24	23	24	23	16	19	17
$3p/4$	SP%	99	99	99	99	100	100	100	100
	SE%	18	17	17	18	15	9	11	9
	MC%	33	33	32	33	33	25	28	24
p	SP%	99	99	99	99	100	100	100	100
	SE%	25	24	23	25	21	13	16	13
	MC%	40	41	40	41	40	31	34	29
$2p$	SP%	99	99	99	99	100	100	100	100
	SE%	49	49	48	51	44	30	35	27
	MC%	63	64	63	65	62	51	55	47

Next, we assess the effectiveness of the refitting technique developed in Section 2.2 for reducing the estimation bias in the magnitude of the non-zero entries. This is accomplished by examining improvements in the relative error of the Frobenius norm, namely $\frac{\|\hat{\Omega} - \Omega^0\|_F}{\|\Omega^0\|_F}$, for the original and refitted estimates. Specifically, let \hat{E} denote the collection of indices selected as non-zero using the thresholding procedure described at the end of Section 2.1, and $\{\hat{\Omega}(t)\}_{t=1}^T$ denote the sequence of iterates obtained by running the Gibbs sampler in Algorithm 1. Our first estimate of Ω is given by

$$\hat{\Omega}_{BSSC} = \begin{cases} \frac{\sum_{t=1}^T \hat{\omega}_{jk}^{(t)}}{\sum_{t=1}^T \mathbf{1}_{\{\hat{\omega}_{jk}^{(t)} \neq 0\}}} & \text{if } (j, k) \in \hat{E}, \text{ or } j = k, \\ 0 & \text{if } (j, k) \notin \hat{E}. \end{cases} \quad (4.2)$$

The second estimate, denoted by $\hat{\Omega}_{refitted}$, is the posterior mean of the refitted posterior density in (2.16), which can again be computed by the modified Gibbs sampling procedure on $\mathbb{M}_{\hat{G}}$ discussed at the end of Section 2.2. Note that both $\hat{\Omega}_{BSSC}$ and $\hat{\Omega}_{refitted}$ set the indices not in \hat{E} to be zero, and differ only in the magnitudes of indices classified as non-zero, i.e., indices in \hat{E} . We consider settings with $p \in (50, 100, 150, 200, \text{ and } 300)$, and $n = p$. The true precision matrix Ω^0 is generated by using the same mechanism as in Section 4.1, and for each p , the relative Frobenius norm of the two estimates described above are averaged

over the 50 replicate data sets. The results are shown in Table 4, and clearly demonstrate the improvement obtained by refitting, especially for larger values of p .

Table 4: Summary of average relative error for estimation of the magnitudes of the precision matrix entries for estimates directly obtained from Algorithm 1 vs. estimates obtained by using the refitting technique in Section 2.2

	$p = n = 50$	$p = n = 100$	$p = n = 150$	$p = n = 200$	$p = n = 300$
BSSC	0.38	0.45	0.45	0.45	0.49
BSSC with refitting	0.36	0.35	0.32	0.32	0.29

4.3 An Application of B-CONCORD to Inflammatory Bowel Disease Metabolomics data

There are a number of factors that impact the stool metabolome, including diet, gut flora and gut function. The data analyzed next come from 208 female subjects with inflammatory bowel disease (IBD) -which includes Crohns disease and ulcerative colitis, affect several million individuals worldwide- that participated in the Integrative Human Microbiome Project (iHMP) and were extracted from the Metabolomics Workbench www.metabolomicsworkbench.org (Study ID ST000923). The data correspond to measurements of 428 primary (directly involved in normal growth, development, and reproduction cellular processes) and secondary (produced by bacteria, fungi, etc.) metabolites and lipids (fatty acids and their derivatives). Specifically, 240 primary, 49 secondary and 139 lipids were profiled by a mass spectrometry analytical platform.

The B-CONCORD methodology was employed to estimate the interaction networks of these compounds and the results are shown in Table 5. It can be seen that there are relatively strong interactions between primary and secondary metabolites and also between primary metabolites and lipids.

Next, we comment on some specific patterns that align with findings in the literature. We observed that the short chain fatty acids (acetate, butyrate and propionate) have a high number of connections (~ 22 on average and significantly higher than other compounds), a result consistent with their function as the main source of energy for cells lining the colon and impacting the latter’s health Wong et al. [2006]. Further, the primary bile acid cholate and its glycine and taurine conjugates (glycocholate, taurocholate), as well as secondary bile acids (lithocholate and deoxycholate), were also strongly connected (~ 15 connections on average) and are known to play a role in IBD Tiratterra et al. [2018], Lavelle and Sokol [2020]. Finally,

	Secondary	Primary	Lipids
Secondary	32	337	65
Primary	337	935	355
Lipids	65	355	412

Table 5: Interactions between primary, secondary metabolites and lipids in IBD specimens

sphingolipids (ceramides, phosphocolines and sphingomyelins) form connected clusters, since they represent structural components of intestinal cell membranes and are also signaling molecules involved in cell fate decisions Abdel Hadi et al. [2016].

In general, the proposed model identifies numerous interesting interactions in this rich data set that could provide insights on how they impact molecular processes in IBD.

5 Discussion

This article proposes a fast scalable Bayesian framework for estimating interaction networks through Gaussian graphical models. The use of a generalized likelihood function in combination with a spike-and-slab prior distribution on the model parameters leads to closed form expressions for the corresponding conditional posterior distributions, thus enabling a fast Gibbs sampler for calculating the posterior distribution. The framework also comes with statistical guarantees on the consistency of the posterior distribution under mild regularity conditions. Another key contribution is the introduction of a modified prior distribution that is applicable to the identified network (graphical model) from the data, which provides improved estimates of the magnitudes of the edges in the interaction network. The provided numerical work renders support to the strong gains in the performance of the methods vis-a-vis competing procedures.

References

- Loubna Abdel Hadi, Clara Di Vito, and Laura Riboni. Fostering inflammatory bowel disease: sphingolipid strategies to join forces. *Mediators of inflammation*, 2016, 2016.
- Yves A Atchadé et al. On the contraction properties of some high-dimensional quasi-posterior distributions. *The Annals of Statistics*, 45(5):2248–2273, 2017.
- Onureena Banerjee, Laurent El Ghaoui, and Alexandre d’Aspremont. Model selection through sparse maximum likelihood estimation for multivariate gaussian or binary data. *Journal of Machine learning research*, 9(Mar):485–516, 2008.
- Sayantana Banerjee and Subhashis Ghosal. Posterior convergence rates for estimating large precision matrices using graphical models. *Electronic Journal of Statistics*, 8(2):2111–2137, 2014.
- Sayantana Banerjee and Subhashis Ghosal. Bayesian structure learning in graphical models. *Journal of Multivariate Analysis*, 136:147–162, 2015.
- J. Besag. Statistical analysis of non-lattice data. *Journal of the Royal Statistical Society: Series D (The Statistician)*, 24:179–195, 1975.
- Anirban Bhattacharya, Debdeep Pati, Natesh S Pillai, and David B Dunson. Dirichlet–laplace priors for optimal shrinkage. *Journal of the American Statistical Association*, 110(512):1479–1490, 2015.

- Peter J Bickel and Elizaveta Levina. Regularized estimation of large covariance matrices. *The Annals of Statistics*, pages 199–227, 2008.
- Peter Bühlmann and Sara Van De Geer. *Statistics for high-dimensional data: methods, theory and applications*. Springer Science & Business Media, 2011.
- T. Cai, W. Liu, and X. Luo. A constrained l1 minimization approach to sparse precision matrix estimation. *Journal of the American Statistical Association*, 106:594–607, 2011.
- Carlos M Carvalho, Nicholas G Polson, and James G Scott. The horseshoe estimator for sparse signals. *Biometrika*, 97(2):465–480, 2010.
- Shizhe Chen, Daniela M Witten, and Ali Shojaie. Selection and estimation for mixed graphical models. *Biometrika*, 102(1):47–64, 2015.
- Y. Cheng and A. Lenkoski. Hierarchical gaussian graphical models: Beyond reversible jump. *Electronic Journal of Statistics*, 6:2309–2331, 2012.
- A. Dobra, A. Lenkoski, and A. Rodriguez. Bayesian inference for general gaussian graphical models with application to multivariate lattice data. *Journal of the American Statistical Association*, 106:1418–1433, 2011.
- Jerome Friedman, Trevor Hastie, and Robert Tibshirani. Sparse inverse covariance estimation with the graphical lasso. *Biostatistics*, 9(3):432–441, 2008.
- A. Javanmard and A. Montanari. Confidence intervals and hypothesis testing for high-dimensional regression. *Journal of Machine Learning Research*, 15:2869–2909, 2014.
- Kshitij Khare, Sang-Yun Oh, and Bala Rajaratnam. A convex pseudolikelihood framework for high dimensional partial correlation estimation with convergence guarantees. *Journal of the Royal Statistical Society: Series B (Statistical Methodology)*, 77(4):803–825, 2015.
- Aonghus Lavelle and Harry Sokol. Gut microbiota-derived metabolites as key actors in inflammatory bowel disease. *Nature Reviews Gastroenterology & Hepatology*, pages 1–15, 2020.
- Jing Ma and George Michailidis. Joint structural estimation of multiple graphical models. *The Journal of Machine Learning Research*, 17(1):5777–5824, 2016.
- Enes Makalic and Daniel F Schmidt. A simple sampler for the horseshoe estimator. *IEEE Signal Processing Letters*, 23(1):179–182, 2016.
- N. Meinshausen and P. Bühlmann. High dimensional graphs and variable selection with the lasso. *Annals of Statistics*, 34:1436–1462, 2006.
- Radford M Neal. Slice sampling. *The annals of statistics*, 31(3):705–767, 2003.
- Henning Omre and Kjetil B Halvorsen. The bayesian bridge between simple and universal kriging. *Mathematical Geology*, 21(7):767–786, 1989.

- Trevor Park and George Casella. The bayesian lasso. *Journal of the American Statistical Association*, 103(482):681–686, 2008.
- Jie Peng, Pei Wang, Nengfeng Zhou, and Ji Zhu. Partial correlation estimation by joint sparse regression models. *Journal of the American Statistical Association*, 104(486):735–746, 2009.
- Nicholas G Polson and James G Scott. Shrink globally, act locally: Sparse bayesian regularization and prediction. *Bayesian statistics*, 9:501–538, 2010.
- Nicholas G Polson and James G Scott. Local shrinkage rules, lévy processes and regularized regression. *Journal of the Royal Statistical Society: Series B (Statistical Methodology)*, 74(2):287–311, 2012.
- Mark Rudelson and Roman Vershynin. Hanson-wright inequality and sub-gaussian concentration. *Electronic Communications in Probability*, 18, 2013.
- Elisa Tiraterra, Placido Franco, Emanuele Porru, Konstantinos H Katsanos, Dimitrios K Christodoulou, and Giulia Roda. Role of bile acids in inflammatory bowel disease. *Annals of gastroenterology*, 31(3):266, 2018.
- Sara Van De Geer. On the asymptotic variance of the debiased lasso. *Electronic Journal of Statistics*, 13:2970–3008, 2019.
- Martin J Wainwright. *High-dimensional statistics: A non-asymptotic viewpoint*, volume 48. Cambridge University Press, 2019.
- Matthew P Wand, John T Ormerod, Simone A Padoan, and Rudolf Frühwirth. Mean field variational bayes for elaborate distributions. *Bayesian Analysis*, 6(4):847–900, 2011.
- H. Wang. Scaling it up: Stochastic search structure learning in graphical models. *Bayesian Analysis*, 10:351–377, 2015.
- Hao Wang et al. Bayesian graphical lasso models and efficient posterior computation. *Bayesian Analysis*, 7(4):867–886, 2012.
- Julia MW Wong, Russell De Souza, Cyril WC Kendall, Azadeh Emam, and David JA Jenkins. Colonic health: fermentation and short chain fatty acids. *Journal of clinical gastroenterology*, 40(3):235–243, 2006.
- Ruoxuan Xiang, Kshitij Khare, and Malay Ghosh. High dimensional posterior convergence rates for decomposable graphical models. *Electronic Journal of Statistics*, 9(2):2828–2854, 2015.
- Ming Yuan and Yi Lin. Model selection and estimation in the gaussian graphical model. *Biometrika*, 94(1):19–35, 2007.
- C.H. Zhang and S. Zhang. Confidence intervals for low dimensional parameters in high dimensional linear models. *Journal of the Royal Statistical Society: Series B (Statistical Methodology)*, 76:217–242, 2014.

S 1 Appendix A: Proof of Theorem 1

By Assumption 3 and the Hanson-Wright inequality [Rudelson and Vershynin, 2013], there exists a $c_1 > 0$, independent of n such that

$$P \left\{ \max_{i,j} \|s_{ij} - \sigma_{ij}\| < c_1 \sqrt{\frac{\log p}{n}} \right\} \geq 1 - \frac{1}{p^2},$$

and,

$$P \left\{ \max_{i,j} \|\mathbf{\Omega}_{:i}^{0'} \mathbf{S}_{:j}\| < c_1 \sqrt{\frac{\log p}{n}} \right\} \geq 1 - \frac{1}{p^2}.$$

Define the events $C_{1,n}$, $C_{2,n}$ as

$$C_{1,n} = \left\{ \max_{i,j} \|s_{ij} - \sigma_{ij}\| < c_1 \sqrt{\frac{\log p}{n}} \right\}, \quad (\text{S } 1.1)$$

$$C_{2,n} = \left\{ \max_{i,j} \|\mathbf{\Omega}_{:i}^{0'} \mathbf{S}_{:j}\| < c_1 \sqrt{\frac{\log p}{n}} \right\}, \quad (\text{S } 1.2)$$

for the next series of lemmas, we restrict ourself to the event $C_{1,n} \cap C_{2,n}$.

The next two lemmas prove important properties of the matrix $\mathbf{\Phi}$ that appears in the generalized posterior distribution.

Lemma S 1. *The following holds*

$$\text{eig}_{\min}(\mathbf{S}) \leq \text{eig}_{\min}(\mathbf{\Phi}) \leq \text{eig}_{\max}(\mathbf{\Phi}) \leq 2\text{eig}_{\max}(\mathbf{S}). \quad (\text{S } 1.3)$$

Proof. Let $\mathbf{y} = \mathbf{y}(\mathbf{\Omega})$ be a vectorized version of $\mathbf{\Omega}$ obtained by shifting the corresponding diagonal entry at the bottom of each column of $\mathbf{\Omega}$ and then stacking the columns on top of each other. Let \mathbf{P}^i be the $p \times p$ permutation matrix such that $\mathbf{P}^i \mathbf{z} = (z_1, \dots, z_{i-1}, z_{i+1}, \dots, z_p, z_i)$ for every $\mathbf{z} \in \mathbb{R}^p$. It follows by the definition of \mathbf{y} that

$$\mathbf{y} = \mathbf{y}(\mathbf{\Omega}) = \left((\mathbf{P}^1 \mathbf{\Omega}_{:1})', (\mathbf{P}^2 \mathbf{\Omega}_{:2})', \dots, (\mathbf{P}^p \mathbf{\Omega}_{:p})' \right)'$$

Let $\mathbf{x} \in \mathbb{R}^{\frac{p(p+1)}{2}}$ be the symmetric version of \mathbf{y} obtained by removing all ω_{ij} with $i > j$. More precisely,

$$\mathbf{x} = (\omega_{11}, \omega_{12}, \omega_{22}, \dots, \omega_{1p}, \dots, \omega_{pp})'$$

Let $\tilde{\mathbf{P}}$ be the $p^2 \times \frac{p(p+1)}{2}$ matrix such that every entry of $\tilde{\mathbf{P}}$ is either zero or one, exactly one entry in each row of $\tilde{\mathbf{P}}$ is equal to 1, and $\mathbf{y} = \tilde{\mathbf{P}} \mathbf{x}$.

Next, define $\boldsymbol{\xi} = (\omega_{12}, \omega_{13}, \dots, \omega_{p-1p})'$ and $\boldsymbol{\delta} = (\omega_{11}, \omega_{22}, \dots, \omega_{pp})'$ and let $\tilde{\mathbf{Q}}$ be the $\frac{p(p+1)}{2} \times \frac{p(p+1)}{2}$ permutation matrix for which

$$\mathbf{x} = \mathbf{Q} \begin{pmatrix} \boldsymbol{\xi} \\ \boldsymbol{\delta} \end{pmatrix}.$$

Let $\tilde{\mathbf{S}}$ be a $p^2 \times p^2$ block diagonal matrix with p diagonal blocks, the i^{th} block is equal to $\tilde{\mathbf{S}}^i := \mathbf{P}^i \mathbf{S} \mathbf{P}^{i'}$. It follows that

$$\begin{aligned} \text{tr} [\Omega^2 \mathbf{S}] &= \sum_{i=1}^p \Omega_{:i}' \mathbf{S} \Omega_{:i} = \sum_{i=1}^p \Omega_{:i}' \mathbf{P}^{i'} \mathbf{P}^i \mathbf{S} \mathbf{P}^{i'} \mathbf{P}^i \Omega_{:i} = \sum_{i=1}^p \Omega_{:i}' \mathbf{P}^{i'} \left(\mathbf{P}^i \mathbf{S} \mathbf{P}^{i'} \right) \mathbf{P}^i \Omega_{:i} \\ &= \mathbf{y}' \tilde{\Sigma} \mathbf{y} = \mathbf{x}' \tilde{\mathbf{P}}' \tilde{\mathbf{S}} \tilde{\mathbf{P}} \mathbf{x} = (\boldsymbol{\xi}', \boldsymbol{\delta}') \mathbf{Q}' \tilde{\mathbf{P}}' \tilde{\mathbf{S}} \tilde{\mathbf{P}} \mathbf{Q} \begin{pmatrix} \boldsymbol{\xi} \\ \boldsymbol{\delta} \end{pmatrix}. \end{aligned}$$

There also exist appropriate matrices \mathbf{A} and \mathbf{D} such that

$$\text{tr} [\Omega^2 \mathbf{S}] = (\boldsymbol{\xi}', \boldsymbol{\delta}') \begin{pmatrix} \boldsymbol{\Phi} & \mathbf{A} \\ \mathbf{A} & \mathbf{D} \end{pmatrix} \begin{pmatrix} \boldsymbol{\xi} \\ \boldsymbol{\delta} \end{pmatrix},$$

therefore, we must have

$$\mathbf{Q}' \tilde{\mathbf{P}}' \tilde{\mathbf{S}} \tilde{\mathbf{P}} \mathbf{Q} = \begin{pmatrix} \boldsymbol{\Phi} & \mathbf{A} \\ \mathbf{A} & \mathbf{D} \end{pmatrix}.$$

Note that since $\tilde{\mathbf{P}}$ has orthogonal columns with ℓ_2 -norm either 1 or 2, and the spectrum of $\tilde{\mathbf{S}}$ and \mathbf{S} are identical, we have that

$$\text{eig}_{\min}(\mathbf{S}) = \text{eig}_{\min}(\tilde{\mathbf{S}}) \leq \text{eig}_{\min}(\boldsymbol{\Phi}) \leq \text{eig}_{\max}(\boldsymbol{\Phi}) \leq 2 \text{eig}_{\max}(\tilde{\mathbf{S}}) = 2 \text{eig}_{\max}(\mathbf{S}).$$

□

Lemma S 2. Let $\mathbf{l} \in \mathcal{L}$ be any sparsity pattern/model with $d_{\mathbf{l}} < \tau_n = \frac{\tilde{\varepsilon}_0}{4c_1} \sqrt{\frac{n}{\log p}}$, then the sub matrix $\boldsymbol{\Phi}_{\mathbf{u}}$ of $\boldsymbol{\Phi}$, obtained by taking out all the rows and columns corresponding to the zero coordinates in $\boldsymbol{\xi} \in \mathcal{M}_{\mathbf{l}}$, is positive definite. Specifically,

$$\frac{3\tilde{\varepsilon}_0}{4} \leq \text{eig}_{\min}(\boldsymbol{\Phi}_{\mathbf{u}}) \leq \text{eig}_{\max}(\boldsymbol{\Phi}_{\mathbf{u}}) \leq \frac{5}{2\tilde{\varepsilon}_0}, \quad \forall \mathbf{l} \in \mathcal{L}. \quad (\text{S } 1.4)$$

Proof. Let $\boldsymbol{\Phi}_{\mathbf{u}}^0$ denote the population version of $\boldsymbol{\Phi}_{\mathbf{u}}$. Since, we are restricted to $C_{1,n} \cap C_{2,n}$, $\|\boldsymbol{\Phi}_{\mathbf{u}} - \boldsymbol{\Phi}_{\mathbf{u}}^0\| \leq c_1 d_{\mathbf{l}} \sqrt{\frac{\log p}{n}}$, hence

$$\begin{aligned} \text{eig}_{\min}(\boldsymbol{\Phi}_{\mathbf{u}}) &= \inf_{|\mathbf{x}|=1} \mathbf{x}' \boldsymbol{\Phi}_{\mathbf{u}} \mathbf{x} \geq \inf_{|\mathbf{x}|=1} \mathbf{x}' \boldsymbol{\Phi}_{\mathbf{u}}^0 \mathbf{x} - \inf_{|\mathbf{x}|=1} \mathbf{x}' (\boldsymbol{\Phi}_{\mathbf{u}} - \boldsymbol{\Phi}_{\mathbf{u}}^0) \mathbf{x} \\ &\geq \inf_{|\mathbf{x}|=1} \mathbf{x}' \boldsymbol{\Phi}_{\mathbf{u}}^0 \mathbf{x} - \|\boldsymbol{\Phi}_{\mathbf{u}} - \boldsymbol{\Phi}_{\mathbf{u}}^0\|_2 \\ &\geq \inf_{|\mathbf{x}|=1} \mathbf{x}' \boldsymbol{\Phi}_{\mathbf{u}}^0 \mathbf{x} - c_1 d_{\mathbf{l}} \sqrt{\frac{\log p}{n}} \end{aligned}$$

hence, by Lemma S 1,

$$\begin{aligned} \text{eig}_{\min}(\boldsymbol{\Phi})_{\mathbf{u}} &\geq \tilde{\varepsilon}_0 - c_1 d_{\mathbf{l}} \sqrt{\frac{\log p}{n}} \\ &\geq \tilde{\varepsilon}_0 - c_1 \tau_n \sqrt{\frac{\log p}{n}} = \frac{3\tilde{\varepsilon}_0}{4}. \end{aligned}$$

Similarly one can show that

$$\text{eig}_{\max}(\Phi u) \leq \frac{5}{2\tilde{\varepsilon}_0}.$$

□

By Lemma S 2, the value of the threshold τ_n which we used in building our hierarchical prior in 2.5 is given as $\tau_n = \frac{\tilde{\varepsilon}_0}{4c_1} \sqrt{\frac{n}{\log p}}$. Hence by Assumption 1, we can write $d_t \leq \tau_n$, for any sufficiently large n .

Lemma S 3. *Let $\boldsymbol{\xi}^0, \boldsymbol{\delta}^0$ be the true values of $\boldsymbol{\xi}, \boldsymbol{\delta}, \Phi$ and $\mathbf{a} = \mathbf{A}\boldsymbol{\delta}^0$ be according to (3.2) and (3.3), and $\hat{\mathbf{a}} = \mathbf{A}\hat{\boldsymbol{\delta}}$ be the estimate of \mathbf{a} obtained by replacing $\boldsymbol{\delta}^0$ by the accurate diagonal estimates $\hat{\boldsymbol{\delta}}$. Then for large enough n , there exists a constant c_0 such that*

$$\|\Phi \boldsymbol{\xi}^0 + \hat{\mathbf{a}}\|_{\max} \leq c_0 \sqrt{\frac{\log p}{n}}. \quad (\text{S } 1.5)$$

Proof. Note that by the triangular inequality,

$$\|\Phi \boldsymbol{\xi}^0 + \hat{\mathbf{a}}\|_{\max} \leq \|\Phi \boldsymbol{\xi}^0 + \mathbf{a}\|_{\max} + \|\hat{\mathbf{a}} - \mathbf{a}\|_{\max}, \quad (\text{S } 1.6)$$

where, provided by Assumption 1.

Next, in view of (3.2), (3.3), and (3.1),

$$\Phi \boldsymbol{\xi}^0 + \mathbf{a} = \begin{pmatrix} \Omega_{:1}^{0'} \mathbf{S}_{:2} + \Omega_{:2}^{0'} \mathbf{S}_{:1} \\ \Omega_{:1}^{0'} \mathbf{S}_{:3} + \Omega_{:3}^{0'} \mathbf{S}_{:1} \\ \vdots \\ \Omega_{:p-1}^{0'} \mathbf{S}_{:p} + \Omega_{:p}^{0'} \mathbf{S}_{:p-1} \end{pmatrix},$$

hence, by restricting to the event $C_{1,n} \cap C_{2,n}$, we have that

$$\begin{aligned} \|\Phi \boldsymbol{\xi}^0 + \mathbf{a}\|_{\max} &\leq \sqrt{\max_{1 \leq i < j \leq p} (\Omega_{:i}^{0'} \mathbf{S}_{:j})^2} \\ &\leq \max_{1 \leq i < j \leq p} |\Omega_{:i}^{0'} (\mathbf{S}_{:j} - \boldsymbol{\Sigma}_{:j})| \\ &\leq 2c_1 \sqrt{\frac{\log p}{n}}. \end{aligned} \quad (\text{S } 1.7)$$

Moreover, by (3.3) and (3.4), it is easy to see that

$$\|\hat{\mathbf{a}} - \mathbf{a}\|_{\max} \leq 2C \|\mathbf{S}\|_{\max} \sqrt{\frac{\log p}{n}}.$$

Since we are restricting to the event $C_{1,n}$, it follows by Assumption 3 that

$$\|\hat{\mathbf{a}} - \mathbf{a}\|_{\max} \leq \frac{5C}{\tilde{\varepsilon}_0} \sqrt{\frac{\log p}{n}} \quad (\text{S } 1.8)$$

By combining (S 1.6), (S 1.7), and (S 1.8), we get that

$$\|\Phi \boldsymbol{\xi}^0 + \hat{\mathbf{a}}\|_{\max} \leq \left(2c_1 + \frac{5C}{\tilde{\varepsilon}_0}\right) \sqrt{\frac{\log p}{n}}.$$

The result follows by letting $c_0 = 2c_1 + \frac{5C}{\tilde{\varepsilon}_0}$. \square

For ease of presentation, we denote the ratio of the posterior probabilities of any sparsity pattern/model \mathbf{l} and the true sparsity pattern/model \mathbf{t} , by $PR(\mathbf{l}, \mathbf{t})$, i.e.

$$PR(\mathbf{l}, \mathbf{t}) = \frac{P\{\mathbf{l}|\hat{\boldsymbol{\delta}}, \mathcal{Y}\}}{P\{\mathbf{t}|\hat{\boldsymbol{\delta}}, \mathcal{Y}\}}, \quad \text{for any sparsity pattern } \mathbf{l} \neq \mathbf{t}. \quad (\text{S } 1.9)$$

Lemma S 4. *The ratio of the posterior probabilities of any sparsity pattern/model \mathbf{l} and the true sparsity pattern/model \mathbf{t} satisfies:*

$$\begin{aligned} PR(\mathbf{l}, \mathbf{t}) &= \frac{\pi\{\mathbf{l}|\hat{\boldsymbol{\delta}}, \mathcal{Y}\}}{\pi\{\mathbf{t}|\hat{\boldsymbol{\delta}}, \mathcal{Y}\}} = \frac{q^{d_l}(1-q)^{\binom{p}{2}-d_l}}{q^{d_t}(1-q)^{\binom{p}{2}-d_t}} \\ &\times \frac{|\Lambda_{\mathbf{l}u}|^{\frac{1}{2}} |(n\Phi + \Lambda)_{tt}|^{\frac{1}{2}} \exp\left\{\frac{n^2}{2} \hat{\mathbf{a}}_l' (n\Phi + \Lambda)_{\mathbf{l}u}^{-1} \hat{\mathbf{a}}_l\right\}}{|\Lambda_{\mathbf{t}t}|^{\frac{1}{2}} |(n\Phi + \Lambda)_{\mathbf{t}t}|^{\frac{1}{2}} \exp\left\{\frac{n^2}{2} \hat{\mathbf{a}}_t' (n\Phi + \Lambda)_{\mathbf{t}t}^{-1} \hat{\mathbf{a}}_t\right\}}. \end{aligned} \quad (\text{S } 1.10)$$

Proof. We note that

$$\pi\{\mathbf{l}|\hat{\boldsymbol{\delta}}, \mathcal{Y}\} = \pi\{\boldsymbol{\xi} \in \mathcal{M}_{\mathbf{l}}|\hat{\boldsymbol{\delta}}, \mathcal{Y}\} = \int_{\mathcal{M}_{\mathbf{l}}} \pi(\boldsymbol{\xi}|\hat{\boldsymbol{\delta}}, \mathcal{Y}) d\boldsymbol{\xi},$$

Hence, in view of (3.5),

$$\pi\{\mathbf{l}|\hat{\boldsymbol{\delta}}, \mathcal{Y}\} = C_0 q^{d_l} (1-q)^{\binom{p}{2}-d_l} \frac{|\Lambda_{\mathbf{l}u}|^{\frac{1}{2}}}{|(n\Phi + \Lambda)_{\mathbf{l}u}|^{\frac{1}{2}}} \exp\left\{\frac{n^2}{2} \hat{\mathbf{a}}_l' (n\Phi + \Lambda)_{\mathbf{l}u}^{-1} \hat{\mathbf{a}}_l\right\},$$

where the last equality is achieved using the properties of the multivariate normal distribution. \square

In the next series of lemmas, we will show that for any sparsity pattern $\mathbf{l} \in \mathcal{L}$, the posterior probability ratio $PR(\mathbf{l}, \mathbf{t})$ is approaching zero, as n goes to ∞ . Specifically, we consider four cases of underfitted ($\mathbf{l} \subset \mathbf{t}$), overfitted ($\mathbf{t} \subset \mathbf{l}$ with $d_l < \tau_n$), and non-inclusive ($\mathbf{t} \not\subseteq \mathbf{l}$ and $\mathbf{l} \not\subseteq \mathbf{t}$) models.

Lemma S 5. *Suppose $\mathbf{l} \subset \mathbf{t}$ then, under Assumptions 1 - 5*

$$PR(\mathbf{l}, \mathbf{t}) \rightarrow 0, \quad \text{as } n \rightarrow \infty. \quad (\text{S } 1.11)$$

Proof. By Assumption 2, $d_t < \tau$, hence $d_l < d_t < \tau$. Now,

$$\begin{aligned} PR(\mathbf{l}, \mathbf{t}) &= \frac{\|\Lambda_{\mathbf{u}}\|^{\frac{1}{2}}}{\|\Lambda_{\mathbf{tt}}\|^{\frac{1}{2}}} \left(\frac{q}{1-q} \right)^{d_l - d_t} \frac{\|(n\Phi + \Lambda)_{\mathbf{tt}}\|^{\frac{1}{2}} \exp \left\{ \frac{n^2}{2} \hat{\mathbf{a}}_l' (n\Phi + \Lambda)_{\mathbf{u}}^{-1} \hat{\mathbf{a}}_l \right\}}{\|(n\Phi + \Lambda)_{\mathbf{u}}\|^{\frac{1}{2}} \exp \left\{ \frac{n^2}{2} \hat{\mathbf{a}}_t' (n\Phi + \Lambda)_{\mathbf{tt}}^{-1} \hat{\mathbf{a}}_t \right\}} \\ &= \frac{\|\Lambda_{\mathbf{u}}\|^{\frac{1}{2}}}{\|\Lambda_{\mathbf{tt}}\|^{\frac{1}{2}}} \left(\frac{q}{1-q} \right)^{d_l - d_t} \frac{\|(n\Phi + \Lambda)_{\mathbf{tt}}\|^{\frac{1}{2}}}{\|(n\Phi + \Lambda)_{\mathbf{u}}\|^{\frac{1}{2}}} \\ &\quad \exp \left\{ -\frac{n^2}{2} [\hat{\mathbf{a}}_{l^c} - n\Phi_{l^c l} (n\Phi + \Lambda)_{\mathbf{u}}^{-1} \hat{\mathbf{a}}_l]' (n\Phi + \Lambda)_{\mathbf{t} \setminus l}^{-1} [\hat{\mathbf{a}}_{l^c} - n\Phi_{l^c l} (n\Phi + \Lambda)_{\mathbf{u}}^{-1} \hat{\mathbf{a}}_l] \right\}, \end{aligned}$$

where $l^c = \mathbf{t} \setminus l$. It follows that

$$PR(\mathbf{l}, \mathbf{t}) \leq \frac{\|\Lambda_{\mathbf{u}}\|^{\frac{1}{2}}}{\|\Lambda_{\mathbf{tt}}\|^{\frac{1}{2}}} \left(\frac{q}{1-q} \right)^{d_l - d_t} \frac{\|(n\Phi + \Lambda)_{\mathbf{tt}}\|^{\frac{1}{2}}}{\|(n\Phi + \Lambda)_{\mathbf{u}}\|^{\frac{1}{2}}} \exp \left\{ -\frac{n^2 \|\hat{\mathbf{a}}_{l^c} - n\Phi_{l^c l} (n\Phi + \Lambda)_{\mathbf{u}}^{-1} \hat{\mathbf{a}}_l\|^2}{2 \text{eig}_{\max}(n\Phi + \Lambda)_{\mathbf{tt}}} \right\},$$

Now, by the triangular inequality,

$$\begin{aligned} &\|\hat{\mathbf{a}}_{l^c} - n\Phi_{l^c l} (n\Phi + \Lambda)_{\mathbf{u}}^{-1} \hat{\mathbf{a}}_l\| \\ &\quad \geq \|\mathbf{a}_{l^c} - n\Phi_{l^c l} (n\Phi + \Lambda)_{\mathbf{u}}^{-1} \mathbf{a}_l\| \\ &\quad \quad - \|(\hat{\mathbf{a}}_{l^c} - \mathbf{a}_{l^c}) - n\Phi_{l^c l} (n\Phi + \Lambda)_{\mathbf{u}}^{-1} (\hat{\mathbf{a}}_l - \mathbf{a}_l)\| \\ &= \|(\pm\Phi\xi^0 + \mathbf{a})_{l^c} - n\Phi_{l^c l} (n\Phi + \Lambda)_{\mathbf{u}}^{-1} (\pm\Phi\xi^0 + \mathbf{a})_l\| \\ &\quad \quad - \|(\hat{\mathbf{a}}_{l^c} - \mathbf{a}_{l^c}) - n\Phi_{l^c l} (n\Phi + \Lambda)_{\mathbf{u}}^{-1} (\hat{\mathbf{a}}_l - \mathbf{a}_l)\| \\ &\geq \|(\Phi\xi^0)_{l^c} - n\Phi_{l^c l} (n\Phi + \Lambda)_{\mathbf{u}}^{-1} (\Phi\xi^0)_l\| \\ &\quad \quad - \|(\Phi\xi^0 + \mathbf{a})_{l^c} - n\Phi_{l^c l} (n\Phi + \Lambda)_{\mathbf{u}}^{-1} (\Phi\xi^0 + \mathbf{a})_l\| \\ &\quad \quad - \|(\hat{\mathbf{a}}_{l^c} - \mathbf{a}_{l^c}) - n\Phi_{l^c l} (n\Phi + \Lambda)_{\mathbf{u}}^{-1} (\hat{\mathbf{a}}_l - \mathbf{a}_l)\|. \end{aligned} \tag{S 1.12}$$

Now, by appropriately partitioning Φ , we can write $(\Phi\xi^0)_{l^c} = \Phi_{l^c l} \xi_l^0 + \Phi_{l^c l^c} \xi_{l^c}^0$ and $(\Phi\xi^0)_l = \Phi_{ll} \xi_l^0 + \Phi_{ll^c} \xi_{l^c}^0$. Hence, for large enough n ,

$$\begin{aligned}
\| (\Phi \xi^0)_{l^c} - n \Phi_{l^c l} (n \Phi + \Lambda)_u^{-1} (\Phi \xi^0)_l \| &= \left\| \frac{1}{n} (n \Phi + \Lambda)_{t|l} \xi_{l^c}^0 - \Phi_{l^c l} (n \Phi + \Lambda)_u^{-1} \Lambda_u \xi_l^0 \right\| \\
&\geq \left\| \frac{1}{n} (n \Phi + \Lambda)_{t|l} \xi_{l^c}^0 \right\| - \left\| \Phi_{l^c l} (n \Phi + \Lambda)_u^{-1} \Lambda_u \xi_l^0 \right\| \\
&\geq \left\| \frac{1}{n} (n \Phi + \Lambda)_{t|l} \xi_{l^c}^0 \right\| - \frac{\text{eig}_{\min}(\Phi_{l^c l}) \|\Lambda_u \xi_l^0\|}{\text{eig}_{\min}(n \Phi + \Lambda)_u} \\
&\geq \left\| \frac{1}{n} (n \Phi + \Lambda)_{t|l} \xi_{l^c}^0 \right\| - \frac{2 \|\Lambda_u \xi_l^0\|}{n \tilde{\varepsilon}_0^2} \\
&\geq \frac{1}{2} \left\| \frac{1}{n} (n \Phi + \Lambda)_{t|l} \xi_{l^c}^0 \right\| \\
&\geq \frac{1}{2} \frac{1}{n} \text{eig}_{\min}(n \Phi + \Lambda)_{tt} s_n \sqrt{(d_t - d_l)} \\
&\geq \frac{1}{2} \frac{1}{n} \text{eig}_{\min}(\Phi)_{tt} s_n \sqrt{(d_t - d_l)} \\
&\geq \frac{3}{8} \tilde{\varepsilon}_0 s_n \sqrt{(d_t - d_l)}
\end{aligned} \tag{S 1.13}$$

Moving onto the second term in the right hand side of (S 1.12),

$$\begin{aligned}
&\| (\Phi \xi^0 + \mathbf{a})_{l^c} - n \Phi_{l^c l} (n \Phi + \Lambda)_u^{-1} (\Phi \xi^0 + \mathbf{a})_l \| \\
&\leq \| (\Phi \xi^0 + \mathbf{a})_{l^c} \| + \| n \Phi_{l^c l} (n \Phi + \Lambda)_u^{-1} (\Phi \xi^0 + \mathbf{a})_l \| \\
&\leq \| (\Phi \xi^0 + \mathbf{a})_{l^c} \| + \frac{n \text{eig}_{\max}(\Phi_{l^c l}) \| (\Phi \xi^0 + \mathbf{a})_l \|}{\text{eig}_{\min}(n \Phi + \Lambda)_u} \\
&\leq \| (\Phi \xi^0 + \mathbf{a})_{l^c} \| + \frac{2 \| (\Phi \xi^0 + \mathbf{a})_l \|}{\tilde{\varepsilon}_0^2} \\
&\leq c_0 \sqrt{\frac{\log p}{n}} \left(\sqrt{d_t - d_l} + \frac{2 \sqrt{d_l}}{\tilde{\varepsilon}_0^2} \right),
\end{aligned} \tag{S 1.14}$$

where the last equality was achieved by Lemma S 3. Further, regarding the third term in the right hand side of (S 1.12) we can express it as

$$\begin{aligned}
\| (\hat{\mathbf{a}}_{l^c} - \mathbf{a}_{l^c}) - n \Phi_{l^c l} (n \Phi + \Lambda)_u^{-1} (\hat{\mathbf{a}}_l - \mathbf{a}_l) \| &\leq \| \hat{\mathbf{a}}_{l^c} - \mathbf{a}_{l^c} \| + \frac{n \text{eig}_{\max}(\Phi_{l^c l}) \| (\hat{\mathbf{a}}_l - \mathbf{a}_l) \|}{\text{eig}_{\min}(n \Phi + \Lambda)_u} \\
&\leq \frac{3C}{\tilde{\varepsilon}_0} \sqrt{\frac{\log p}{n}} \left(\sqrt{d_t - d_l} + \frac{2 \sqrt{d_l}}{\tilde{\varepsilon}_0^2} \right),
\end{aligned} \tag{S 1.15}$$

Hence, by combining (S 1.12), (S 1.13), (S 1.14), and (S 1.15), for sufficiently large n , we

have that

$$\begin{aligned}
\|\hat{\mathbf{a}}_{\mathbf{l}^c} - n\Phi_{\mathbf{l}^c\mathbf{l}}(n\Phi + \Lambda)_u^{-1} \hat{\mathbf{a}}_{\mathbf{l}}\| &\geq \frac{3}{8}\tilde{\varepsilon}_0 s_n \sqrt{(d_{\mathbf{t}} - d_{\mathbf{l}})} \\
&\quad - c_0 \sqrt{\frac{\log p}{n}} \left(\sqrt{d_{\mathbf{t}} - d_{\mathbf{l}}} + \frac{2\sqrt{d_{\mathbf{l}}}}{\tilde{\varepsilon}_0^2} \right) \\
&\quad - \frac{3C}{\tilde{\varepsilon}_0} \sqrt{\frac{\log p}{n}} \left(\sqrt{d_{\mathbf{t}} - d_{\mathbf{l}}} + \frac{2\sqrt{d_{\mathbf{l}}}}{\tilde{\varepsilon}_0^2} \right) \\
&\geq \frac{1}{2}\tilde{\varepsilon}_0 s_n \sqrt{(d_{\mathbf{t}} - d_{\mathbf{l}})} \\
&\quad - \left(c_0 + \frac{3C}{\tilde{\varepsilon}_0} \right) \sqrt{\frac{\log p}{n}} \left(\sqrt{d_{\mathbf{t}} - d_{\mathbf{l}}} + \frac{2\sqrt{d_{\mathbf{l}}}}{\tilde{\varepsilon}_0^2} \right) \\
&\geq \frac{1}{2}\tilde{\varepsilon}_0 s_n - \left(c_0 + \frac{3C}{\tilde{\varepsilon}_0} \right) \sqrt{\frac{\log p}{n}} \left(\frac{2\sqrt{d_{\mathbf{t}}}}{\tilde{\varepsilon}_0^2} \right),
\end{aligned}$$

in view of Assumption 5, $\frac{\frac{3}{8}\tilde{\varepsilon}_0 s_n}{\left(c_0 + \frac{3C}{\tilde{\varepsilon}_0}\right) \sqrt{\frac{\log p}{n}} \left(\frac{2\sqrt{d_{\mathbf{t}}}}{\tilde{\varepsilon}_0^2}\right)} \rightarrow \infty$, as $n \rightarrow \infty$, hence, for all large n , we can write,

$$\|\hat{\mathbf{a}}_{\mathbf{l}^c} - n\Phi_{\mathbf{l}^c\mathbf{l}}(n\Phi + \Lambda)_u^{-1} \hat{\mathbf{a}}_{\mathbf{l}}\| \geq \frac{1}{4}\tilde{\varepsilon}_0 s_n$$

Now, once again by Lemma S 3

$$\begin{aligned}
PR(\mathbf{l}, \mathbf{t}) &\leq \frac{\|\Lambda_{\mathbf{u}\mathbf{u}}\|^{\frac{1}{2}}}{\|\Lambda_{\mathbf{t}\mathbf{t}}\|^{\frac{1}{2}}} (2q)^{d_{\mathbf{l}} - d_{\mathbf{t}}} n^{\frac{d_{\mathbf{t}} - d_{\mathbf{l}}}{2}} \exp \left\{ -\frac{n^2 \frac{1}{64} \tilde{\varepsilon}_0^2 s_n^2}{6n\tilde{\varepsilon}_0^{-1}} \right\} \\
&= \frac{\|\Lambda_{\mathbf{u}\mathbf{u}}\|^{\frac{1}{2}}}{\|\Lambda_{\mathbf{t}\mathbf{t}}\|^{\frac{1}{2}}} 2^{d_{\mathbf{l}} - d_{\mathbf{t}}} \left(\frac{\sqrt{n}}{q} \exp \left\{ -\frac{n\tilde{\varepsilon}_0^3 s_n^2}{384} \right\} \right)^{d_{\mathbf{t}} - d_{\mathbf{l}}}.
\end{aligned}$$

Since the diagonal entries of Λ are uniformly bounded, it follows by Assumption 4 that for large enough n

$$\begin{aligned}
PR(\mathbf{l}, \mathbf{t}) &\leq \frac{\|\Lambda_{\mathbf{u}\mathbf{u}}\|^{\frac{1}{2}}}{\|\Lambda_{\mathbf{t}\mathbf{t}}\|^{\frac{1}{2}}} 2^{d_{\mathbf{l}} - d_{\mathbf{t}}} \left(\frac{\sqrt{n}}{q} \exp \{ -\log n - 2a_2 d_{\mathbf{t}} \log p \} \right)^{d_{\mathbf{t}} - d_{\mathbf{l}}} \\
&= \frac{\|\Lambda_{\mathbf{u}\mathbf{u}}\|^{\frac{1}{2}}}{\|\Lambda_{\mathbf{t}\mathbf{t}}\|^{\frac{1}{2}}} 2^{d_{\mathbf{l}} - d_{\mathbf{t}}} \left(\frac{p^{-2a_2 d_{\mathbf{t}}}}{\sqrt{n}q} \right)^{d_{\mathbf{t}} - d_{\mathbf{l}}} \\
&= \frac{\|\Lambda_{\mathbf{u}\mathbf{u}}\|^{\frac{1}{2}}}{\|\Lambda_{\mathbf{t}\mathbf{t}}\|^{\frac{1}{2}}} 2^{d_{\mathbf{l}} - d_{\mathbf{t}}} \left(\frac{p^{-a_2 d_{\mathbf{t}}}}{\sqrt{n}} \right)^{d_{\mathbf{t}} - d_{\mathbf{l}}} \\
&= \left(\frac{2C_1 p^{-a_2 d_{\mathbf{t}}}}{\sqrt{n}} \right)^{d_{\mathbf{t}} - d_{\mathbf{l}}}
\end{aligned}$$

where C_1 is an appropriate constant. □

Lemma S 6. *Suppose $\mathbf{l} \supset \mathbf{t}$, and $d_{\mathbf{l}} < \tau_n$ then, under Assumptions 1 - 5*

$$PR(\mathbf{l}, \mathbf{t}) \rightarrow 0, \quad \text{as } n \rightarrow \infty.$$

Proof. In this case,

$$PR(\mathbf{l}, \mathbf{t}) = \frac{\|\mathbf{\Lambda}_{\mathbf{u}}\|^{\frac{1}{2}}}{\|\mathbf{\Lambda}_{\mathbf{tt}}\|^{\frac{1}{2}} \|(n\mathbf{\Phi} + \mathbf{\Lambda})_{\mathbf{l}|\mathbf{t}}\|^{\frac{1}{2}}} (2q)^{d_{\mathbf{l}} - d_{\mathbf{t}}} \exp \left\{ \frac{n^2}{2} \hat{\mathbf{a}}_{\mathbf{l}}' (n\mathbf{\Phi} + \mathbf{\Lambda})_{\mathbf{u}}^{-1} \hat{\mathbf{a}}_{\mathbf{l}} - \frac{n^2}{2} \hat{\mathbf{a}}_{\mathbf{t}}' (n\mathbf{\Phi} + \mathbf{\Lambda})_{\mathbf{tt}}^{-1} \hat{\mathbf{a}}_{\mathbf{t}} \right\}.$$

Using the fact that $\boldsymbol{\xi}_{\mathbf{l}|\mathbf{t}}^0 = \mathbf{0}$, we get

$$\begin{aligned} & [(n\mathbf{\Phi} + \mathbf{\Lambda})_{\mathbf{u}} \boldsymbol{\xi}_{\mathbf{l}}^0 + n\hat{\mathbf{a}}_{\mathbf{l}}]' (n\mathbf{\Phi} + \mathbf{\Lambda})_{\mathbf{u}}^{-1} [(n\mathbf{\Phi} + \mathbf{\Lambda})_{\mathbf{u}} \boldsymbol{\xi}_{\mathbf{l}}^0 + n\hat{\mathbf{a}}_{\mathbf{l}}] - n^2 \hat{\mathbf{a}}_{\mathbf{l}}' (n\mathbf{\Phi} + \mathbf{\Lambda})_{\mathbf{u}}^{-1} \hat{\mathbf{a}}_{\mathbf{l}} \\ &= 2n (\boldsymbol{\xi}_{\mathbf{l}}^0)' \hat{\mathbf{a}}_{\mathbf{l}} + (\boldsymbol{\xi}_{\mathbf{l}}^0)' (n\mathbf{\Phi} + \mathbf{\Lambda})_{\mathbf{u}} (\boldsymbol{\xi}_{\mathbf{l}}^0) \\ &= 2n (\boldsymbol{\xi}_{\mathbf{t}}^0)' \hat{\mathbf{a}}_{\mathbf{t}} + (\boldsymbol{\xi}_{\mathbf{t}}^0)' (n\mathbf{\Phi} + \mathbf{\Lambda})_{\mathbf{tt}} (\boldsymbol{\xi}_{\mathbf{t}}^0) \\ &= [(n\mathbf{\Phi} + \mathbf{\Lambda})_{\mathbf{tt}} \boldsymbol{\xi}_{\mathbf{t}}^0 + n\hat{\mathbf{a}}_{\mathbf{t}}]' (n\mathbf{\Phi} + \mathbf{\Lambda})_{\mathbf{tt}}^{-1} [(n\mathbf{\Phi} + \mathbf{\Lambda})_{\mathbf{tt}} \boldsymbol{\xi}_{\mathbf{t}}^0 + n\hat{\mathbf{a}}_{\mathbf{t}}] - n^2 \hat{\mathbf{a}}_{\mathbf{t}}' (n\mathbf{\Phi} + \mathbf{\Lambda})_{\mathbf{tt}}^{-1} \hat{\mathbf{a}}_{\mathbf{t}} \\ &\geq -n^2 \hat{\mathbf{a}}_{\mathbf{t}}' (n\mathbf{\Phi} + \mathbf{\Lambda})_{\mathbf{tt}}^{-1} \hat{\mathbf{a}}_{\mathbf{t}}. \end{aligned}$$

It follows that

$$PR(\mathbf{l}, \mathbf{t}) \leq \frac{\|\mathbf{\Lambda}_{\mathbf{u}}\|^{\frac{1}{2}}}{\|\mathbf{\Lambda}_{\mathbf{tt}}\|^{\frac{1}{2}} \|(n\mathbf{\Phi} + \mathbf{\Lambda})_{\mathbf{l}|\mathbf{t}}\|^{\frac{1}{2}}} (2q)^{d_{\mathbf{l}} - d_{\mathbf{t}}} \exp \left\{ \frac{1}{2} [(n\mathbf{\Phi} + \mathbf{\Lambda})_{\mathbf{u}} \boldsymbol{\xi}_{\mathbf{l}}^0 + n\hat{\mathbf{a}}_{\mathbf{l}}]' (n\mathbf{\Phi} + \mathbf{\Lambda})_{\mathbf{u}}^{-1} [(n\mathbf{\Phi} + \mathbf{\Lambda})_{\mathbf{u}} \boldsymbol{\xi}_{\mathbf{l}}^0 + n\hat{\mathbf{a}}_{\mathbf{l}}] \right\}.$$

Now, we note by Lemma S 3 that each entry of

$$(n\mathbf{\Phi} + \mathbf{\Lambda})_{\mathbf{u}} \boldsymbol{\xi}_{\mathbf{l}}^0 + n\hat{\mathbf{a}}_{\mathbf{l}} = n (\mathbf{\Phi} \boldsymbol{\xi}^0 + \mathbf{a})_{\mathbf{l}} + \mathbf{\Lambda}_{\mathbf{u}} \boldsymbol{\xi}_{\mathbf{l}}^0, +n (\hat{\mathbf{a}} - \mathbf{a})_{\mathbf{l}}$$

is smaller in absolute value than

$$nc_0 \sqrt{\frac{\log p}{n}} + \frac{\|\mathbf{\Lambda}\|_{\max}}{\tilde{\varepsilon}_0} + \frac{3C}{\tilde{\varepsilon}_0} \sqrt{\frac{\log p}{n}} \leq \frac{3nc_0}{2} \sqrt{\frac{\log p}{n}},$$

hence, by Lemma S 2,

$$\begin{aligned} & [(n\mathbf{\Phi} + \mathbf{\Lambda})_{\mathbf{u}} \boldsymbol{\xi}_{\mathbf{l}}^0 + n\hat{\mathbf{a}}_{\mathbf{l}}]' (n\mathbf{\Phi} + \mathbf{\Lambda})_{\mathbf{u}}^{-1} [(n\mathbf{\Phi} + \mathbf{\Lambda})_{\mathbf{u}} \boldsymbol{\xi}_{\mathbf{l}}^0 + n\hat{\mathbf{a}}_{\mathbf{l}}] \\ &\leq \frac{1}{n\tilde{\varepsilon}_0} d_{\mathbf{l}} \frac{4n^2 c_0^2 \log p}{n} = \frac{4c_0^2 d_{\mathbf{l}} \log p}{\tilde{\varepsilon}_0}. \end{aligned}$$

Hence,

$$\begin{aligned}
PR(\mathbf{l}, \mathbf{t}) &\leq \frac{\|\Lambda_{\mathbf{ll}}\|^{\frac{1}{2}} (2q)^{d_{\mathbf{l}}-d_{\mathbf{t}}}}{\|\Lambda_{\mathbf{tt}}\|^{\frac{1}{2}} \left(\frac{n\tilde{\varepsilon}_0}{2}\right)^{\frac{d_{\mathbf{l}}-d_{\mathbf{t}}}{2}}} \exp\left\{\frac{2c_0^2}{\tilde{\varepsilon}_0} d_{\mathbf{l}} \log p\right\} \\
&= \frac{2^{d_{\mathbf{l}}-d_{\mathbf{t}}} \|\Lambda_{\mathbf{ll}}\|^{\frac{1}{2}} q^{d_{\mathbf{l}}-d_{\mathbf{t}}} p^{\frac{2c_0^2 d_{\mathbf{l}}}{\tilde{\varepsilon}_0}}}{\|\Lambda_{\mathbf{tt}}\|^{\frac{1}{2}} \left(\frac{n\tilde{\varepsilon}_0}{2}\right)^{\frac{d_{\mathbf{l}}-d_{\mathbf{t}}}{2}}} \\
&\leq \frac{2^{d_{\mathbf{l}}-d_{\mathbf{t}}} \|\Lambda_{\mathbf{ll}}\|^{\frac{1}{2}}}{\|\Lambda_{\mathbf{tt}}\|^{\frac{1}{2}} \left(\frac{n\tilde{\varepsilon}_0}{2}\right)^{\frac{d_{\mathbf{l}}-d_{\mathbf{t}}}{2}}} p^{-a_2 d_{\mathbf{t}}(d_{\mathbf{l}}-d_{\mathbf{t}})+a_2 d_{\mathbf{l}}/4} \\
&= \frac{2^{d_{\mathbf{l}}-d_{\mathbf{t}}} \|\Lambda_{\mathbf{ll}}\|^{\frac{1}{2}}}{\|\Lambda_{\mathbf{tt}}\|^{\frac{1}{2}} \left(\frac{n\tilde{\varepsilon}_0}{2}\right)^{\frac{d_{\mathbf{l}}-d_{\mathbf{t}}}{2}}} \left(p^{-a_2 d_{\mathbf{t}}+a_2 \frac{d_{\mathbf{l}}}{4(d_{\mathbf{l}}-d_{\mathbf{t}})}}\right)^{d_{\mathbf{l}}-d_{\mathbf{t}}} \\
&= \frac{2^{d_{\mathbf{l}}-d_{\mathbf{t}}} \|\Lambda_{\mathbf{ll}}\|^{\frac{1}{2}}}{\|\Lambda_{\mathbf{tt}}\|^{\frac{1}{2}} \left(\frac{n\tilde{\varepsilon}_0}{2}\right)^{\frac{d_{\mathbf{l}}-d_{\mathbf{t}}}{2}}} \left(p^{-a_2 d_{\mathbf{t}}+a_2 \frac{d_{\mathbf{l}}}{2}}\right)^{d_{\mathbf{l}}-d_{\mathbf{t}}} \\
&\leq \left(\frac{4C_1 p^{-\frac{a_2 d_{\mathbf{t}}}{2}}}{\sqrt{n\tilde{\varepsilon}_0}}\right)^{d_{\mathbf{l}}-d_{\mathbf{t}}} \tag{S 1.16}
\end{aligned}$$

for an appropriate constant C_2 . □

Lemma S 7. *Let $\mathbf{l} \in \mathcal{L}$ such that $\mathbf{l} \not\subseteq \mathbf{t}$, $\mathbf{t} \not\subseteq \mathbf{l}$, $\mathbf{l} \neq \mathbf{t}$ and $d_{\mathbf{l}} \leq \tau_n$, then under Assumptions 1 - 5 for sufficiently large n ,*

$$PR(\mathbf{l}, \mathbf{t}) \rightarrow 0, \quad \text{as } n \rightarrow \infty.$$

Proof. By using the formula for the inverse of a partitioned matrix, it can be shown that

$$\begin{pmatrix} \mathbf{x}'_1 & \mathbf{x}'_2 \end{pmatrix} \begin{pmatrix} \mathbf{A}_{11} & \mathbf{A}_{12} \\ \mathbf{A}'_{12} & \mathbf{A}_{22} \end{pmatrix}^{-1} \begin{pmatrix} \mathbf{x}_1 \\ \mathbf{x}_2 \end{pmatrix} - \mathbf{x}'_1 \mathbf{A}_{11}^{-1} \mathbf{x}_1 = (\mathbf{x}_2 - \mathbf{A}'_{12} \mathbf{A}_{11}^{-1} \mathbf{x}_1)' \mathbf{F}^{-1} (\mathbf{x}_2 - \mathbf{A}'_{12} \mathbf{A}_{11}^{-1} \mathbf{x}_1) \geq 0, \tag{S 1.17}$$

where $\mathbf{F} = \mathbf{A}_{22} - \mathbf{A}'_{12} \mathbf{A}_{11}^{-1} \mathbf{A}_{12}$.

Suppose \mathbf{l} is such that $d_{\mathbf{l}} > d_{\mathbf{t}}$. Let $\tilde{\mathbf{l}}$ denote the union of \mathbf{l} and \mathbf{t} . Then $\tilde{\mathbf{l}} \supset \mathbf{t}$ and

$$d_{\tilde{\mathbf{l}}} \leq d_{\mathbf{l}} + d_{\mathbf{t}} \leq \tau_n + d_{\mathbf{t}}.$$

As in the proof of Lemma S 6, using the fact $\xi_{\tilde{\mathbf{l}} \setminus \mathbf{t}} = \mathbf{0}$ and (S 1.17), we get that

$$\begin{aligned}
&n^2 \hat{\mathbf{a}}'_{\mathbf{l}} (n\Phi + \Lambda)_{\tilde{\mathbf{l}}\tilde{\mathbf{l}}}^{-1} \hat{\mathbf{a}}_{\mathbf{l}} - n^2 \hat{\mathbf{a}}'_{\mathbf{t}} (n\Phi + \Lambda)_{\tilde{\mathbf{l}}\tilde{\mathbf{l}}}^{-1} \hat{\mathbf{a}}_{\mathbf{t}} \\
&\leq n^2 \hat{\mathbf{a}}'_{\mathbf{l}} (n\Phi + \Lambda)_{\tilde{\mathbf{l}}\tilde{\mathbf{l}}}^{-1} \hat{\mathbf{a}}_{\mathbf{l}} - n^2 \hat{\mathbf{a}}'_{\mathbf{t}} (n\Phi + \Lambda)_{\tilde{\mathbf{l}}\tilde{\mathbf{l}}}^{-1} \hat{\mathbf{a}}_{\mathbf{t}} \\
&\leq [(n\Phi + \Lambda)_{\tilde{\mathbf{l}}\tilde{\mathbf{l}}} \xi_{\tilde{\mathbf{l}}\tilde{\mathbf{l}}}^0 + n\hat{\mathbf{a}}_{\tilde{\mathbf{l}}}]' (n\Phi + \Lambda)_{\tilde{\mathbf{l}}\tilde{\mathbf{l}}}^{-1} [(n\Phi + \Lambda)_{\tilde{\mathbf{l}}\tilde{\mathbf{l}}} \xi_{\tilde{\mathbf{l}}\tilde{\mathbf{l}}}^0 + n\hat{\mathbf{a}}_{\tilde{\mathbf{l}}}] - \\
&\quad [(n\Phi + \Lambda)_{\mathbf{tt}} \xi_{\mathbf{tt}}^0 + n\hat{\mathbf{a}}_{\mathbf{t}}]' (n\Phi + \Lambda)_{\mathbf{tt}}^{-1} [(n\Phi + \Lambda)_{\mathbf{tt}} \xi_{\mathbf{tt}}^0 + n\hat{\mathbf{a}}_{\mathbf{t}}] \\
&\leq \frac{4c_0^2 d_{\tilde{\mathbf{l}}} \log p}{\tilde{\varepsilon}_0} \leq \frac{4c_0^2 (d_{\mathbf{l}} + d_{\mathbf{t}}) \log p}{\tilde{\varepsilon}_0}
\end{aligned}$$

It follows that

$$\begin{aligned}
PR(\mathbf{l}, \mathbf{t}) &\leq \frac{\|\Lambda_{\mathbf{U}}\|^{\frac{1}{2}} (2q)^{d_l-d_t}}{\|\Lambda_{\mathbf{t}\mathbf{t}}\|^{\frac{1}{2}} \left(\frac{n\tilde{\varepsilon}_0}{2}\right)^{\frac{d_l-d_t}{2}}} \exp\left\{\frac{2C_0^2}{\tilde{\varepsilon}_0}(d_l+d_t)\log p\right\} \\
&= \frac{2^{d_l-d_t}\|\Lambda_{\mathbf{U}}\|^{\frac{1}{2}} q^{d_l-d_t} p^{\frac{2c_0^2(d_l+d_t)}{\tilde{\varepsilon}_0}}}{\|\Lambda_{\mathbf{t}\mathbf{t}}\|^{\frac{1}{2}} \left(\frac{n\tilde{\varepsilon}_0}{2}\right)^{\frac{d_l-d_t}{2}}} \\
&= \frac{2^{d_l-d_t}\|\Lambda_{\mathbf{U}}\|^{\frac{1}{2}}}{\|\Lambda_{\mathbf{t}\mathbf{t}}\|^{\frac{1}{2}} \left(\frac{n\tilde{\varepsilon}_0}{2}\right)^{\frac{d_l-d_t}{2}}} \left(p^{-a_2 d_t + a_2 \frac{d_l+d_t}{4(d_l-d_t)}}\right)^{d_l-d_t} \\
&= \frac{2^{d_l-d_t}\|\Lambda_{\mathbf{U}}\|^{\frac{1}{2}}}{\|\Lambda_{\mathbf{t}\mathbf{t}}\|^{\frac{1}{2}} \left(\frac{n\tilde{\varepsilon}_0}{2}\right)^{\frac{d_l-d_t}{2}}} \left(p^{-a_2 d_t + a_2 \frac{3d_t}{4}}\right)^{d_l-d_t} \\
&\leq \left(\frac{4C_2 p^{-\frac{a_2 d_t}{4}}}{\sqrt{n\tilde{\varepsilon}_0}}\right)^{d_l-d_t} \tag{S 1.18}
\end{aligned}$$

where C_2 is as in the proof of Lemma S 6. Let $D(\mathbf{l}, \mathbf{t})$ denotes the total number of disagreements between \mathbf{l} and \mathbf{t} . Note that if $d_l > d_t$, then

$$D(\mathbf{l}, \mathbf{t}) \leq 2d_t(d_l - d_t).$$

Hence

$$PR(\mathbf{l}, \mathbf{t}) \leq \left(\frac{4C_2 p^{-\frac{a_2}{8}}}{\sqrt{n\tilde{\varepsilon}_0}}\right)^{D(\mathbf{l}, \mathbf{t})}.$$

Suppose \mathbf{l} is such that $d_l \leq d_t$. Note that

$$\begin{aligned}
&\hat{\mathbf{a}}'_l (n\Phi + \Lambda)_{\mathbf{U}}^{-1} \hat{\mathbf{a}}_l - \hat{\mathbf{a}}'_t (n\Phi + \Lambda)_{\mathbf{t}\mathbf{t}}^{-1} \hat{\mathbf{a}}_t \\
&= \hat{\mathbf{a}}'_l \left((n\Phi + \Lambda)_{\mathbf{U}}^{-1} - (n\Phi)_{\mathbf{U}}^{-1} \right) \hat{\mathbf{a}}_l - \hat{\mathbf{a}}'_t \left((n\Phi + \Lambda)_{\mathbf{t}\mathbf{t}}^{-1} - (n\Phi)_{\mathbf{t}\mathbf{t}}^{-1} \right) \hat{\mathbf{a}}_t + \\
&\quad \frac{1}{n} \hat{\mathbf{a}}'_l (\Phi)_{\mathbf{U}}^{-1} \hat{\mathbf{a}}_l - \frac{1}{n} \hat{\mathbf{a}}'_t (\Phi)_{\mathbf{t}\mathbf{t}}^{-1} \hat{\mathbf{a}}_t \\
&= O\left(\frac{d_t}{n^2}\right) + \frac{1}{n} \hat{\mathbf{a}}'_l (\Phi)_{\mathbf{U}}^{-1} \hat{\mathbf{a}}_l - \frac{1}{n} \hat{\mathbf{a}}'_t (\Phi)_{\mathbf{t}\mathbf{t}}^{-1} \hat{\mathbf{a}}_t
\end{aligned}$$

and by Lemma S 3

$$(\Phi\xi^0 + \hat{\mathbf{a}})'_l (\Phi)_{\mathbf{U}}^{-1} (\Phi\xi^0 + \hat{\mathbf{a}})_l + (\Phi\xi^0 + \hat{\mathbf{a}})'_t (\Phi)_{\mathbf{t}\mathbf{t}}^{-1} (\Phi\xi^0 + \hat{\mathbf{a}})_t = O\left(\frac{d_t \log p}{n}\right)$$

on $C_{1,n}$. Let \mathbf{l}^c denote the sparsity pattern which has a zero/one whenever the corresponding entry in \mathbf{l} is one/zero. Using $\xi_{\mathbf{l}^c}^0 = \mathbf{0}$ and Lemma S 2, it follows that

$$\begin{aligned}
&(\Phi\xi^0)'_l (\Phi)_{\mathbf{U}}^{-1} (\Phi\xi^0)_l - (\Phi\xi^0)'_t (\Phi)_{\mathbf{t}\mathbf{t}}^{-1} (\Phi\xi^0)_t \\
&= \xi_{\mathbf{l}}^{0'} \Phi_{\mathbf{U}} \xi_{\mathbf{l}}^0 + \xi_{\mathbf{l}}^{0'} \Phi_{\mathbf{U}^c} \xi_{\mathbf{l}^c}^0 + \xi_{\mathbf{l}^c}^{0'} \Phi_{\mathbf{l}^c} \Phi_{\mathbf{U}}^{-1} \Phi_{\mathbf{U}^c} \xi_{\mathbf{l}^c}^0 - \xi_{\mathbf{t}}^{0'} \Phi_{\mathbf{t}\mathbf{t}} \xi_{\mathbf{t}}^0 \\
&= \xi_{\mathbf{l}}^{0'} \Phi \xi_{\mathbf{l}}^0 - \xi_{\mathbf{l}^c}^{0'} \Phi_{\mathbf{l}^c} \xi_{\mathbf{l}^c}^0 - \xi_{\mathbf{l}^c}^{0'} (\Phi_{\mathbf{l}^c} - \Phi_{\mathbf{l}^c} \Phi_{\mathbf{U}}^{-1} \Phi_{\mathbf{U}^c}) \xi_{\mathbf{l}^c}^0 \\
&\leq -\frac{3d_{\mathbf{l}^c} \tilde{\varepsilon}_0 s_n^2}{4},
\end{aligned}$$

since exactly $d_{t \cap l^c}$ entries in $\boldsymbol{\xi}_{l^c}^0$ are non-zero. Since $d_{t \cap l^c} \geq d_t - d_l$ and $D(\mathbf{l}, \mathbf{t}) \leq 2d_t$ similar arguments to those at the end of Lemma S 5 can be used to obtain

$$PR(\mathbf{l}, \mathbf{t}) \leq \left(\frac{2C_1 p^{-a_2 d_t}}{\sqrt{n}} \right)^{d_{t \cap l^c}} \leq \left(\frac{2C_1 p^{-a_2/2}}{\sqrt{n}} \right)^{D(\mathbf{l}, \mathbf{t})}.$$

□

It follows by Lemmas S 5, S 6 and S 7 that for every $\mathbf{l} \neq \mathbf{t}$ with $d_l \leq \tau_n$,

$$PR(\mathbf{l}, \mathbf{t}) \leq f_n^{D(\mathbf{l}, \mathbf{t})}$$

where

$$f_n = \max \left\{ \left(\frac{2C_1 p^{-a_2/2}}{\sqrt{n}} \right), \left(\frac{4C_2 p^{-\frac{a_2}{8}}}{\sqrt{n \hat{\varepsilon}_0}} \right) \right\}.$$

The first part of Theorem 1 a is straightforward application of Lemmas S 5, S 6, and S 7. Note that $a_2 \geq 16$, which implies $p^2 f_n \rightarrow 0$ as $n \rightarrow \infty$. It follows that

$$\begin{aligned} \frac{1 - P \left\{ \boldsymbol{\xi} \in \mathcal{M}_t | \hat{\boldsymbol{\delta}}, \mathcal{Y} \right\}}{P \left\{ \boldsymbol{\xi} \in \mathcal{M}_t | \hat{\boldsymbol{\delta}}, \mathcal{Y} \right\}} &= \sum_{\mathbf{l} \neq \mathbf{t}} PR(\mathbf{l}, \mathbf{t}) \\ &= \sum_{\mathbf{l} \neq \mathbf{t}} \sum_{j=1}^{\binom{p}{2}} PR(\mathbf{l}, \mathbf{t}) I_{\{D(\mathbf{l}, \mathbf{t})=j\}} \\ &\leq \sum_{j=1}^{\binom{p}{2}} \binom{\binom{p}{2}}{j} f_n^j \\ &\leq \sum_{j=1}^{\binom{p}{2}} \binom{p}{2}^j f_n^j \\ &\leq \sum_{j=1}^{p^2} (p^2 f_n)^j \\ &\leq \frac{p^2 f_n}{1 - p^2 f_n} \rightarrow 0 \quad \text{as } n \rightarrow \infty. \end{aligned} \tag{S 1.19}$$

on $C_{1,n}$. Since $\mathbb{P}_0(C_{1,n}) \rightarrow 1$ as $n \rightarrow \infty$, we get that

$$\pi \left\{ \mathbf{t} | \hat{\boldsymbol{\delta}}, \mathcal{Y} \right\} \xrightarrow{\mathbb{P}_0} 1, \quad \text{as } n \rightarrow \infty.$$

We now prove the second part of Theorem 1. For every pair (j, k) , let π_{jk} denote the posterior probability that ω_{jk} is non-zero. Note that

$$\pi_{jk} \geq \pi \left\{ \mathbf{t} | \hat{\boldsymbol{\delta}}, \mathcal{Y} \right\}$$

for $(j, k) \in E^0$, and

$$\pi_{jk} \leq 1 - \pi \left\{ \mathbf{t} | \hat{\boldsymbol{\delta}}, \mathcal{Y} \right\}$$

for $(j, k) \notin E^0$. It follows by the first part of Theorem 1 that

$$\begin{aligned} \mathbb{P}_0 \left(\hat{\mathbf{t}}_{v, BSSC} = \mathbf{t} \right) &= \mathbb{P}_0 \left(\left\{ \bigcap_{(j,k): (j,k) \in E^0} \{ \pi_{jk} \geq v \} \right\} \cap \left\{ \bigcap_{(j,k): (j,k) \notin E^0} \{ \pi_{jk} < v \} \right\} \right) \\ &\geq \mathbb{P}_0 \left(\pi \left\{ \mathbf{t} | \hat{\boldsymbol{\delta}}, \mathcal{Y} \right\} \geq \max \left(v, 1 - \frac{v}{2} \right) \right) \rightarrow 1 \quad \text{as } n \rightarrow \infty. \end{aligned}$$

S 2 Appendix B: Proofs of Lemmas 1 and 2

Proof of Lemma 1

Note that any principal submatrix of \mathbf{S} of size less than n is positive definite. Let $\lambda > 0$ be the smallest number in the collection of eigenvalues of all principal submatrices of S of size less than n . By assumption, if $\boldsymbol{\Omega} \in \mathbb{M}_{\hat{G}}$, then the i^{th} column of $\boldsymbol{\Omega}$, denoted by $\boldsymbol{\Omega}_{\cdot i}$, has at most $n - 1$ zeros. It follows that

$$\begin{aligned} &\int_{\mathbb{M}_{\hat{G}}} \exp \left\{ n \text{tr}(\boldsymbol{\Omega}) - \frac{n}{2} \text{tr}(\boldsymbol{\Omega}^2 \mathbf{S}) \right\} d\boldsymbol{\Omega} \\ &= \int_{\mathbb{M}_{\hat{G}}} \exp \left\{ n \text{tr}(\boldsymbol{\Omega}) - \frac{n}{2} \sum_{i=1}^n \boldsymbol{\Omega}_{\cdot i}^t \mathbf{S} \boldsymbol{\Omega}_{\cdot i} \right\} d\boldsymbol{\Omega} \\ &\leq \int_{\mathbb{M}_{\hat{G}}} \exp \left\{ n \text{tr}(\boldsymbol{\Omega}) - \frac{n\lambda}{2} \sum_{i=1}^n \boldsymbol{\Omega}_{\cdot i}^t \boldsymbol{\Omega}_{\cdot i} \right\} d\boldsymbol{\Omega} \\ &= \int_{\mathbb{R}^{|\hat{E}|} \times \mathbb{R}_+^p} \exp \left\{ n \sum_{i=1}^p \omega_{ii} - \frac{n\lambda}{2} \sum_{i=1}^p \sum_{j=1}^p \omega_{ij}^2 \right\} \prod_{i < j, (i,j) \in \hat{E}} d\omega_{ij} \\ &= \left(\prod_{i=1}^p \int_{\mathbb{R}_+} \exp \left\{ n\omega_{ii} - \frac{n\lambda}{2} \omega_{ii}^2 \right\} d\omega_{ii} \right) \left(\prod_{i < j, (i,j) \in \hat{E}} \int_{\mathbb{R}} \exp \left\{ -n\lambda \omega_{ij}^2 \right\} d\omega_{ij} \right) \\ &< \infty. \end{aligned}$$

Proof of Lemma 2

Let $\boldsymbol{\omega}_{\hat{G}}$ denote the vectorized version of the non-zero entries in $\boldsymbol{\Omega} \in \mathbb{M}_{\hat{G}}$. It follows that

$$h(\boldsymbol{\omega}_{\hat{G}}) = \frac{n}{2} \text{tr}(\boldsymbol{\Omega}^2 \mathbf{K}^{-1}) - n \text{tr}(\boldsymbol{\Omega}) = \frac{n}{2} \boldsymbol{\omega}'_{\hat{G}} \tilde{K} \boldsymbol{\omega}_{\hat{G}} - n \boldsymbol{\omega}'_{\hat{G}} \mathbf{u},$$

for an appropriate matrix \tilde{K} and an appropriate vector \mathbf{u} . By a similar analysis as in the proof of Lemma S 1, it can be shown that the eigenvalues of \tilde{K} are bounded below by the smallest eigenvalue of K^{-1} . It follows that \tilde{K} is invertible and $h(\boldsymbol{\omega}_{\hat{G}})$ is uniquely minimized at $\tilde{K}^{-1} \mathbf{u}$. Note that for $(i, j) \in \hat{E}$,

$$\frac{\partial}{\partial \omega_{ij}} h(\boldsymbol{\omega}_{\hat{G}}) = n \sum_{i'=1}^p \omega_{i'j} K_{ii'}^{-1} + n \sum_{j'=1}^p \omega_{ij'} K_{jj'}^{-1},$$

and

$$\frac{\partial}{\partial \omega_{ii}} h(\boldsymbol{\omega}_{\hat{G}}) = n \sum_{i'=1}^p \omega_{ii'} K_{ii'}^{-1} - n$$

for $1 \leq i \leq p$. It follows that the vectorized version of the non-zero entries (corresponding to entries in \hat{E}) of the matrix \mathbf{K} satisfies the above first derivative equations, and must coincide with the unique minimum $\tilde{K}^{-1}\mathbf{u}$. Since $\mathbf{K} \in \mathbb{M}_{\hat{G}}$, the result follows.

S 3 Appendix C: Proof of Theorem 2

Note by the definition of \hat{G} in (2.14) and Theorem 1 that

$$\mathbb{P}_0(\hat{G} = G^0) = \mathbb{P}_0(\hat{\mathbf{t}}_{v,BSSC} = \mathbf{t}) \rightarrow 1$$

as $n \rightarrow \infty$. For ease of presentation, let $\epsilon_n = \sqrt{\frac{(p+d_t)\log p}{n}}$. First note that for any constant K' ,

$$\begin{aligned} & \mathbb{E}_0 \left[\pi_{refitted} \left(\|\boldsymbol{\Omega} - \boldsymbol{\Omega}^0\|_{\max} > K' \nu_{\max} \sqrt{d_t \frac{\log p}{n}} \mid \mathcal{Y} \right) \right] \\ & \leq \mathbb{E}_0 \left[\pi_{refitted} \left(\|\boldsymbol{\Omega} - \boldsymbol{\Omega}^0\|_{\max} > K' \nu_{\max} \sqrt{\frac{d_t \log p}{n}} \mid \mathcal{Y} \right) 1_{\{\hat{G}=G^0\}} \right] + \mathbb{P}_0(G \neq G^0) \end{aligned} \quad \text{S 3.1}$$

Hence, it is sufficient to prove that $\mathbb{E}_0 \left[\pi_{refitted} \left(\|\boldsymbol{\Omega} - \boldsymbol{\Omega}^0\|_{FM} > K \sqrt{\frac{\log p}{n}} \mid \mathcal{Y} \right) 1_{\{\hat{G}=G^0\}} \right]$ as $n \rightarrow \infty$. As in the proof of Lemma 2, let $\boldsymbol{\omega}$ denote the vectorized version of the non-zero entries in $\boldsymbol{\Omega} \in \mathbb{M}_{G^0}$, such that the first p entries of $\boldsymbol{\omega}$ correspond to the diagonal entries of $\boldsymbol{\Omega}$, and the last d_t entries of $\boldsymbol{\omega}$ correspond to the (structurally) non-zero off-diagonal entries of $\boldsymbol{\Omega}$. Similarly, let $\boldsymbol{\omega}^0$ denote the vectorized version of the non-zero entries in $\boldsymbol{\Omega} \in \mathbb{M}_{G^0}$. It follows that

$$h(\boldsymbol{\omega}) = \frac{n}{2} \text{tr}(\boldsymbol{\Omega}^2 S) - n \text{tr}(\boldsymbol{\Omega}) = \frac{n}{2} \boldsymbol{\omega}' \tilde{\mathbf{K}} \boldsymbol{\omega} - n \boldsymbol{\omega}' \mathbf{u},$$

for an appropriate matrix \tilde{K} and an appropriate vector \mathbf{u} . It can be shown by straightforward calculations that the first p entries of \mathbf{u} (corresponding to the diagonals) are 1, and the rest are 0. By a similar analysis as in the proof of Lemma S 1, it can be shown that

$$\tilde{\mathbf{K}} = \mathbf{Q}'_t \tilde{\mathbf{P}}'_t \tilde{\mathbf{S}}_t \tilde{\mathbf{P}}_t \mathbf{Q}_t, \quad \text{(S 3.2)}$$

wherein $\tilde{\mathbf{S}}_t$ is a block diagonal matrix with p blocks. For every $1 \leq i \leq p$, the i^{th} block is a principal sub-matrix of the sample covariance matrix S corresponding to indices which are neighbors of i in G^0 , $\tilde{\mathbf{P}}_t$ is an appropriate $(p+2d_t) \times (p+d_t)$ matrix of zeros and ones such that each row has exactly one entry equal to 1, and each column has at most 2 entries equal to 1, and \mathbf{Q}_t is an appropriate $(p+d_t) \times (p+d_t)$ permutation matrix. It follows from (S 3.2) and the structure of $\tilde{\mathbf{P}}_t$ that $\lambda_{\min}(\tilde{\mathbf{K}}) \geq \lambda_{\min}(\tilde{\mathbf{S}}_t)$. Note that $\tilde{\mathbf{S}}_t$ is a block diagonal matrix, and each diagonal block is a sub-matrix of the sample covariance matrix \mathbf{S} of size less than

d_t . It follows by Assumption 3 that on $C_{1,n}$, $\lambda_{\min}(\tilde{\mathbf{S}}_t) \geq \tilde{\varepsilon}_0 - d_t \sqrt{\frac{\log p}{n}} \geq \tilde{\varepsilon}_0/2$ for large enough n . Hence, $\tilde{\mathbf{K}}$ is invertible, and the function $h(\boldsymbol{\omega})$ is uniquely minimized at $\hat{\boldsymbol{\omega}} = \tilde{\mathbf{K}}^{-1}\mathbf{u}$.

Note that by Lemma 2, the function $h_0(\boldsymbol{\omega})$ defined by

$$h_0(\boldsymbol{\omega}) = \frac{n}{2} \text{tr}(\boldsymbol{\Omega}^2 \boldsymbol{\Sigma}^0) - n \text{tr}(\boldsymbol{\Omega}) = \frac{n}{2} \boldsymbol{\omega}' \tilde{\mathbf{K}}^0 \boldsymbol{\omega} - n \boldsymbol{\omega}' \mathbf{u}$$

is uniquely minimized at $\boldsymbol{\omega}^0$. It can be shown that $\boldsymbol{\omega}^0 = (\tilde{\mathbf{K}}^0)^{-1}\mathbf{u}$, where $\tilde{\mathbf{K}} = \mathbf{Q}'_t \tilde{\mathbf{P}}'_t \tilde{\boldsymbol{\Sigma}}_t \tilde{\mathbf{P}}_t \mathbf{Q}_t$, and $\tilde{\boldsymbol{\Sigma}}_t$ is a block diagonal matrix with p blocks. For every $1 \leq i \leq p$, the i^{th} block is a principal sub-matrix of the true covariance matrix $\boldsymbol{\Sigma}^0$ corresponding to indices which are neighbors of i in G^0 .

Next, we show that on $C_{1,n}$, $\|\hat{\boldsymbol{\omega}} - \boldsymbol{\omega}^0\|_{\max} \leq K' \sqrt{d_t \frac{\log p}{n}}$ for a large enough constant K' (not depending on n). Let $d = \{(i, j) : 1 \leq i = j \leq p\}$, $o = \{(i, j) : i < j, (i, j) \in E^0\}$ and $\bar{o} = \{(i, j) : i > j, (i, j) \in E^0\}$. Note that $|d| = p$, and $|o| = |\bar{o}| = d_t$. After straightforward calculations, it can be shown that

$$\tilde{\mathbf{K}} = \begin{pmatrix} \tilde{\mathbf{S}}_{t,dd} & \tilde{\mathbf{S}}_{t,do} + \tilde{\mathbf{S}}_{t,d\bar{o}} \\ \tilde{\mathbf{S}}_{t,od} + \tilde{\mathbf{S}}_{t,\bar{o}d} & \tilde{\mathbf{S}}_{t,oo} + \tilde{\mathbf{S}}_{t,\bar{o}\bar{o}} \end{pmatrix} \text{ and } \tilde{\mathbf{K}}^0 = \begin{pmatrix} \tilde{\boldsymbol{\Sigma}}_{t,dd} & \tilde{\boldsymbol{\Sigma}}_{t,do} + \tilde{\boldsymbol{\Sigma}}_{t,d\bar{o}} \\ \tilde{\boldsymbol{\Sigma}}_{t,od} + \tilde{\boldsymbol{\Sigma}}_{t,\bar{o}d} & \tilde{\boldsymbol{\Sigma}}_{t,oo} + \tilde{\boldsymbol{\Sigma}}_{t,\bar{o}\bar{o}} \end{pmatrix},$$

wherein $\tilde{\mathbf{S}}_{t,do}$ denotes the sub-matrix of $\tilde{\mathbf{S}}$ corresponding to the rows in d and columns in o . Other sub-matrices are similarly defined.

Using the form of the inverse of a partitioned matrix, along with $\hat{\boldsymbol{\omega}} = \tilde{\mathbf{K}}^{-1}\mathbf{u}$ and $\boldsymbol{\omega}^0 = (\tilde{\mathbf{K}}^0)^{-1}\mathbf{u}$, it follows that for every $1 \leq i \leq p$, we have

$$\hat{\omega}_{ii} = \mathbf{e}'_i \tilde{\mathbf{S}}_{t,dd}^{-1} \mathbf{1}_p + \mathbf{e}'_i \tilde{\mathbf{S}}_{t,dd}^{-1} (\tilde{\mathbf{S}}_{t,do} + \tilde{\mathbf{S}}_{t,d\bar{o}}) \tilde{\mathbf{S}}_{Schur}^{-1} (\tilde{\mathbf{S}}_{t,od} + \tilde{\mathbf{S}}_{t,\bar{o}d}) \tilde{\mathbf{S}}_{t,dd}^{-1} \mathbf{1}_p,$$

and

$$\omega_{ii}^0 = \mathbf{e}'_i \tilde{\boldsymbol{\Sigma}}_{t,dd}^{-1} \mathbf{1}_p + \mathbf{e}'_i \tilde{\boldsymbol{\Sigma}}_{t,dd}^{-1} (\tilde{\boldsymbol{\Sigma}}_{t,do} + \tilde{\boldsymbol{\Sigma}}_{t,d\bar{o}}) \tilde{\boldsymbol{\Sigma}}_{Schur}^{-1} (\tilde{\boldsymbol{\Sigma}}_{t,od} + \tilde{\boldsymbol{\Sigma}}_{t,\bar{o}d}) \tilde{\boldsymbol{\Sigma}}_{t,dd}^{-1} \mathbf{1}_p.$$

Here \mathbf{e}_i is the i^{th} unit vector in \mathbb{R}^p , $\mathbf{1}_p \in \mathbb{R}^p$ has all entries equal to 1, and $\tilde{\mathbf{S}}_{Schur}$ and $\tilde{\boldsymbol{\Sigma}}_{Schur}$ are the lower principal $d_t \times d_t$ submatrices of $\tilde{\mathbf{K}}^{-1}$ and $(\tilde{\mathbf{K}}^0)^{-1}$ respectively. We now make the following observations using the structure of $\tilde{\mathbf{S}}$ and $\tilde{\boldsymbol{\Sigma}}$.

1. Since $\tilde{\mathbf{S}}_{t,dd}$ and $\tilde{\boldsymbol{\Sigma}}_{t,dd}$ are diagonal matrices with diagonal entries $\{S_{ii}\}_{i=1}^p$ and $\{\Sigma_{ii}^0\}_{i=1}^p$ respectively, it follows that

$$\left| \mathbf{e}'_i \tilde{\mathbf{S}}_{t,dd}^{-1} \mathbf{1}_p - \mathbf{e}'_i \tilde{\boldsymbol{\Sigma}}_{t,dd}^{-1} \mathbf{1}_p \right| = \left| \frac{1}{S_{ii}} - \frac{1}{\Sigma_{ii}^0} \right| \leq K'_1 \sqrt{\frac{\log p}{n}}$$

and

$$\left\| \mathbf{e}'_i \tilde{\mathbf{S}}_{t,dd}^{-1} - \mathbf{e}'_i \tilde{\boldsymbol{\Sigma}}_{t,dd}^{-1} \right\| = \left| \frac{1}{S_{ii}} - \frac{1}{\Sigma_{ii}^0} \right| \leq K'_1 \sqrt{\frac{\log p}{n}}$$

on $C_{1,n}$ for a large enough constant K'_1 .

2. Using Assumption 3 along with the structure of $\tilde{\mathbf{P}}_t$, $\tilde{\mathbf{S}}_t$ and $\tilde{\mathbf{\Sigma}}_t$, we get that for large enough n

$$\|\tilde{\mathbf{S}}_{t,do} + \tilde{\mathbf{S}}_{t,d\bar{o}}\| \leq \|\tilde{\mathbf{K}}\| \leq 2\lambda_{\max}(\tilde{\mathbf{S}}_t) \leq \frac{4}{\tilde{\varepsilon}_0}$$

and

$$\|\tilde{\mathbf{\Sigma}}_{t,do} + \tilde{\mathbf{\Sigma}}_{t,d\bar{o}}\| \leq \|\tilde{\mathbf{K}}^0\| \leq 2\lambda_{\max}(\tilde{\mathbf{\Sigma}}_t) \leq \frac{2}{\tilde{\varepsilon}_0},$$

on $C_{1,n}$. Also, since each structurally non-zero entry of $\tilde{\mathbf{S}}$ and $\tilde{\mathbf{\Sigma}}$ is an appropriate entry of \mathbf{S} and $\mathbf{\Sigma}^0$ respectively, each row of $\tilde{\mathbf{S}}_{t,do} + \tilde{\mathbf{S}}_{t,d\bar{o}}$ and $\tilde{\mathbf{\Sigma}}_{t,do} + \tilde{\mathbf{\Sigma}}_{t,d\bar{o}}$ has at most ν_{\max} non-zero entries, and each column of $\tilde{\mathbf{S}}_{t,do} + \tilde{\mathbf{S}}_{t,d\bar{o}}$ and $\tilde{\mathbf{\Sigma}}_{t,do} + \tilde{\mathbf{\Sigma}}_{t,d\bar{o}}$ has at most 2 non-zero entries, it follows that for large enough n and a large enough constant K'_2

$$\|\tilde{\mathbf{S}}_{t,do} + \tilde{\mathbf{S}}_{t,d\bar{o}} - \tilde{\mathbf{\Sigma}}_{t,do} - \tilde{\mathbf{\Sigma}}_{t,d\bar{o}}\| \leq K'_2 \sqrt{\frac{\nu_{\max} \log p}{n}}$$

on $C_{1,n}$.

3. It can be shown using the structure of $\tilde{\mathbf{S}}_t$ and $\tilde{\mathbf{\Sigma}}_t$ that $(\tilde{\mathbf{S}}_{t,od} + \tilde{\mathbf{S}}_{t,\bar{o}d})\tilde{\mathbf{S}}_{t,dd}^{-1}\mathbf{1}_p$ and $(\tilde{\mathbf{\Sigma}}_{t,od} + \tilde{\mathbf{\Sigma}}_{t,\bar{o}d})\tilde{\mathbf{\Sigma}}_{t,dd}^{-1}\mathbf{1}_p$ are both d_t -dimensional vectors with the entry corresponding to $(i, j) \in E^0$ given by $2S_{ij}^{-1}(S_{ii}^{-1} + S_{jj}^{-1})$ and $2\Sigma_{ij}^0((\Sigma_{ii}^0)^{-1} + (\Sigma_{jj}^0)^{-1})$ respectively. It follows that for large enough n and a large enough constant K'_3

$$\left\| (\tilde{\mathbf{S}}_{t,od} + \tilde{\mathbf{S}}_{t,\bar{o}d})\tilde{\mathbf{S}}_{t,dd}^{-1}\mathbf{1}_p \right\| \leq K'_3\sqrt{d_t}, \quad \left\| (\tilde{\mathbf{\Sigma}}_{t,od} + \tilde{\mathbf{\Sigma}}_{t,\bar{o}d})\tilde{\mathbf{\Sigma}}_{t,dd}^{-1}\mathbf{1}_p \right\| \leq K'_3\sqrt{d_t}$$

and

$$\left\| (\tilde{\mathbf{S}}_{t,od} + \tilde{\mathbf{S}}_{t,\bar{o}d})\tilde{\mathbf{S}}_{t,dd}^{-1}\mathbf{1}_p - (\tilde{\mathbf{\Sigma}}_{t,od} + \tilde{\mathbf{\Sigma}}_{t,\bar{o}d})\tilde{\mathbf{\Sigma}}_{t,dd}^{-1}\mathbf{1}_p \right\| \leq K'_3\sqrt{\frac{d_t \log p}{n}}$$

on $C_{1,n}$.

4. Using Assumption 3 along with the structure of $\tilde{\mathbf{P}}_t$, $\tilde{\mathbf{S}}_t$ and $\tilde{\mathbf{\Sigma}}_t$, we get that for large enough n

$$\|\tilde{\mathbf{S}}_{Schur}\| \leq \|\tilde{\mathbf{K}}^{-1}\| \leq \frac{2}{\tilde{\varepsilon}_0}$$

and

$$\|\tilde{\mathbf{\Sigma}}_{Schur}\| \leq \|(\tilde{\mathbf{K}}^0)^{-1}\| \leq \frac{1}{\tilde{\varepsilon}_0}$$

on $C_{1,n}$. Using

$$\tilde{\mathbf{S}}_{Schur}^{-1} = (\tilde{\mathbf{\Sigma}}_{t,oo} + \tilde{\mathbf{\Sigma}}_{t,\bar{o}\bar{o}}) - (\tilde{\mathbf{\Sigma}}_{t,od} + \tilde{\mathbf{\Sigma}}_{t,\bar{o}d})\tilde{\mathbf{\Sigma}}_{t,dd}^{-1}(\tilde{\mathbf{\Sigma}}_{t,do} + \tilde{\mathbf{\Sigma}}_{t,d\bar{o}})$$

$$\tilde{\mathbf{\Sigma}}_{Schur}^{-1} = (\tilde{\mathbf{\Sigma}}_{t,oo} + \tilde{\mathbf{\Sigma}}_{t,\bar{o}\bar{o}}) - (\tilde{\mathbf{\Sigma}}_{t,od} + \tilde{\mathbf{\Sigma}}_{t,\bar{o}d})\tilde{\mathbf{\Sigma}}_{t,dd}^{-1}(\tilde{\mathbf{\Sigma}}_{t,do} + \tilde{\mathbf{\Sigma}}_{t,d\bar{o}}),$$

along with the fact that $\tilde{\mathbf{S}}_{t,oo} + \tilde{\mathbf{S}}_{t,\bar{o}\bar{o}}$ and $\tilde{\Sigma}_{t,oo} + \tilde{\Sigma}_{t,\bar{o}\bar{o}}$ have at most $2\nu_{\max}$ structurally non-zero entries in each row (and column), we get that for large enough n and a large enough constant K'_4

$$\left\| \tilde{\mathbf{S}}_{Schur} - \tilde{\Sigma}_{Schur} \right\| \leq \nu_{\max} \sqrt{\frac{\log p}{n}}$$

on $C_{1,n}$.

Using the observations above, it follows that for $K' > 2 \max(K'_1, K'_2, K'_3, K'_4)$, and large enough n

$$\max_{1 \leq i \leq p} |\hat{\omega}_{ii} - \omega_{ii}^0| \leq \frac{K'}{2} \nu_{\max} \sqrt{\frac{d_t \log p}{n}} \quad (\text{S 3.3})$$

on $C_{1,n}$.

Now, for every $(i, j) \in E^0$, using the form of the inverse of a partitioned matrix, along with $\hat{\boldsymbol{\omega}} = \tilde{\mathbf{K}}^{-1} \mathbf{u}$ and $\boldsymbol{\omega}^0 = (\tilde{\mathbf{K}}^0)^{-1} \mathbf{u}$, we get that

$$\hat{\omega}_{ij} = \mathbf{v}'_{ij} \tilde{\mathbf{S}}_{Schur} (\tilde{\mathbf{S}}_{t,od} + \tilde{\mathbf{S}}_{t,\bar{o}d}) \tilde{\mathbf{S}}_{t,dd}^{-1} \mathbf{1}_p,$$

and

$$\omega_{ii}^0 = \mathbf{v}'_{ij} \tilde{\Sigma}_{Schur} (\tilde{\Sigma}_{t,od} + \tilde{\Sigma}_{t,\bar{o}d}) \tilde{\Sigma}_{t,dd}^{-1} \mathbf{1}_p$$

for an appropriate unit vector $\mathbf{v}_{ij} \in \mathbb{R}^{d_t}$. Using the observations in 3. and 4. above, it follows that for large enough n

$$\max_{(i,j) \in E^0} |\hat{\omega}_{ij} - \omega_{ij}^0| \leq \frac{K'}{2} \nu_{\max} \sqrt{\frac{d_t \log p}{n}} \quad (\text{S 3.4})$$

on $C_{1,n}$. Since $\mathbb{P}_0(C_{1,n}) \rightarrow 0$ as $n \rightarrow \infty$, using (S 3.1), it is sufficient to prove that

$$\mathbb{E}_0 \left[\pi_{refitted} \left(\|\boldsymbol{\omega} - \hat{\boldsymbol{\omega}}\|_{\max} > K' \nu_{\max} \sqrt{\frac{d_t \log p}{n}} \mid \mathcal{Y} \right) \mathbf{1}_{\{\hat{G}=G^0\}} \right] \rightarrow 0$$

as $n \rightarrow \infty$. It follows from (2.16) and the definition of $\mathbb{M}_{\hat{G}}$ that

$$\begin{aligned} & \pi_{refitted} \left(\|\boldsymbol{\omega} - \hat{\boldsymbol{\omega}}\|_{\max} > K' \nu_{\max} \sqrt{\frac{d_t \log p}{n}} \mid \mathcal{Y} \right) \mathbf{1}_{\{\hat{G}=G^0\}} \\ &= P \left(\|\mathbf{Z}\|_{\max} > K' \nu_{\max} \sqrt{\frac{d_t \log p}{n}} \mid Z_i > -\hat{\omega}_{ii}, \forall 1 \leq i \leq p \right) \\ &\leq \frac{P \left(\|\mathbf{Z}\|_{\max} > K' \nu_{\max} \sqrt{\frac{d_t \log p}{n}} \right)}{P(Z_i > -\hat{\omega}_{ii}, \forall 1 \leq i \leq p)}. \end{aligned} \quad (\text{S 3.5})$$

where P is a probability measure, and the $(p + d_t)$ -dimensional random vector \mathbf{Z} has a multivariate normal distribution with mean $\mathbf{0}$ and covariance matrix $\frac{\tilde{\mathbf{K}}^{-1}}{n}$ under P . Using Assumption 3, the structure of $\tilde{\mathbf{P}}_t, \tilde{\mathbf{S}}_t$, along with (S 3.3), we get that for large enough n

$$\hat{\omega}_{ii} > \frac{\tilde{\varepsilon}_0}{2} \quad \forall 1 \leq i \leq p$$

and

$$\lambda_{\max} \left(\tilde{\mathbf{K}}^{-1} \right) < \frac{2}{\tilde{\varepsilon}_0}$$

on $C_{1,n}$. It follows by the union-sum inequality that

$$\begin{aligned} \frac{P \left(\|\mathbf{Z}\|_{\max} > K' \nu_{\max} \sqrt{\frac{d_t \log p}{n}} \right)}{P(Z_i > -\hat{\omega}_{ii}, \forall 1 \leq i \leq p)} &\leq \frac{\sum_{i=1}^{p+d_t} P \left(|Z_i| > K' \nu_{\max} \sqrt{\frac{d_t \log p}{n}} \right)}{1 - \sum_{i=1}^p P(Z_i < -\hat{\omega}_{ii})} \\ &\leq \frac{\sum_{i=1}^{p+d_t} P \left(|\tilde{Z}_i| > K' \nu_{\max} \sqrt{\frac{\tilde{\varepsilon}_0 d_t \log p}{2}} \right)}{1 - \sum_{i=1}^p P(|Z_i| > \frac{\varepsilon}{2})} \\ &\leq \frac{\sum_{i=1}^{p+d_t} P \left(|\tilde{Z}_i| > K' \nu_{\max} \sqrt{\frac{\tilde{\varepsilon}_0 d_t \log p}{2}} \right)}{1 - \sum_{i=1}^p P \left(|\tilde{Z}_i| > \sqrt{\frac{n \tilde{\varepsilon}_0^3}{8}} \right)}. \end{aligned}$$

where \tilde{Z}_i has a standard normal distribution under the probability measure P for every $1 \leq i \leq p + d_t$. Using Markov's inequality with an appropriate function of \tilde{Z}_i , we get

$$\frac{P \left(\|\mathbf{Z}\|_{\max} > K' \nu_{\max} \sqrt{\frac{d_t \log p}{n}} \right)}{P(Z_i > -\hat{\omega}_{ii}, \forall 1 \leq i \leq p)} \leq \frac{2(p + d_t) \exp(- (K')^2 \nu_{\max}^2 \varepsilon d_t \log p / 4)}{1 - 2p \exp(-n \tilde{\varepsilon}_0^3 / 16)}$$

on $C_{1,n}$. It follows by Assumption 6, (S 3.5), and $\mathbb{P}_0(C_{1,n}) \rightarrow 0$ as $n \rightarrow \infty$ that

$$\mathbb{E}_0 \left[\pi_{refitted} \left(\|\boldsymbol{\omega} - \hat{\boldsymbol{\omega}}\|_{\max} > K' \nu_{\max} \sqrt{\frac{d_t \log p}{n}} \mid \mathcal{Y} \right) 1_{\{\hat{G}=G^0\}} \right] \rightarrow 0$$

as $n \rightarrow \infty$ for a large enough choice of K' . This establishes the first part of Theorem 2 (with the $\|\cdot\|_{\max}$ norm). The second part follows by noting that on $\hat{G} = G^0$

$$\|\boldsymbol{\Omega} - \boldsymbol{\Omega}^0\| \leq \nu_{\max} \|\boldsymbol{\Omega} - \boldsymbol{\Omega}^0\|_{\max}.$$

S 4 Appendix D: Continuous shrinkage priors - Horseshoe prior

Continuous shrinkage prior distributions are a popular alternative to spike-and-slab ones. Such prior distributions have a peak at zero and their tails decay at an appropriate rate. They serve as continuous approximations to the discrete mixture-based spike-and-slab prior distributions. Continuous shrinkage prior distributions are often a scale mixture of normals, such as Laplace-half-Cauchy, etc. (see Polson and Scott [2010], Bhattacharya et al. [2015] and references therein). In the context of linear regression, the Bayesian lasso of Park and Casella [2008], based on the interpretation of the well-known lasso estimator of the regression

coefficients as the posterior mode in a Bayesian model which puts independent Laplace priors on the individual coefficients, has gained popularity in recent years.

As mentioned in Section S 5, the Bayesian Graphical lasso was proposed by Wang et al. [2012], as a Bayesian adaptation of the graphical lasso. The authors in Wang et al. [2012] consider a Bayesian model which puts independent Laplace priors on the off-diagonal entries of Ω and independent exponential priors on the diagonal entries of Ω (restricted to Ω begin positive definite). It follows that the graphical lasso estimator is the posterior mode of this Bayesian model. The Bayesian graphical lasso interpretation immediately yields credible regions for the graphical lasso estimate of Ω . Such estimates of uncertainty are not readily available in the frequentist setting. Alternatively, some practitioners also determine sparsity in Ω based on whether zero is contained in the credible interval for the respective off-diagonal entries.

In principal, any continuous shrinkage prior distribution on the off-diagonal entries can be used in conjunction with the CONCORD generalized likelihood (2.1). We will demonstrate this by choosing the popular horseshoe prior developed in Carvalho et al. [2010]. Consider the following hierarchical prior for every ω_{jk} with $j \neq k$:

$$\begin{aligned}\omega_{jk} | \lambda_{jk}^2, \tau^2 &\sim \mathcal{N}(0, \lambda_{jk}^2 \tau^2), \\ \lambda_{jk} &\sim \mathcal{C}^+(0, 1), \\ \tau &\sim \mathcal{C}^+(0, 1),\end{aligned}\tag{S 4.1}$$

where, \mathcal{C}^+ is the standard half-Cauchy distribution with probability density function

$$p(z) = \frac{2}{\pi(1+z^2)}, \quad z > 0,\tag{S 4.2}$$

and $1 \leq j < k \leq p$.

This hierarchical setting defines the horseshoe prior distribution, which is a global-local shrinkage distribution, wherein the local shrinkage for ω_{jks} is determined by λ_{jks} and the overall level of shrinkage is determined by the hyperparameter τ . The particular choice of the half-Cauchy distribution results in aggressive shrinkage of small in magnitude partial correlations and virtually no shrinkage of the sufficiently large ones. This is in contrast to other continuous shrinkage prior distributions, such as the Laplace (the Bayesian Lasso by Park and Casella [2008]) wherein the shrinkage effect is uniform across all values of the models parameters. For further studies regarding other properties of the horseshoe prior distribution, we refer the reader to Carvalho et al. [2010], Polson and Scott [2012] and Polson and Scott [2010].

Employing the original form of the horseshoe distribution in (S 4.1) results in non-standard conditional posterior distributions for the hyperparameters $\lambda_{12}, \dots, \lambda_{p-1p}, \tau$, which makes a standard Gibbs sampling algorithm difficult to implement. In the context of linear regression models, some studies have suggested the use of specialized algorithms, such as slice sampling for the hyperparameters, Neal [2003] and Omre and Halvorsen [1989]. Recently, Makalic and Schmidt [2016] introduced an alternative sampling scheme for all model parameters based on auxiliary variables that leads to conjugate conditional posterior distributions for all parameters in various regression models. They make use of the following scale

mixture representation of the Horse Shoe prior to construct a Gibbs sampler. Let x and a be random variables such that

$$x^2 \sim \mathcal{IG}(1/2, 1/a), \quad a \sim \mathcal{IG}(1/2, 1/A^2); \quad (\text{S } 4.3)$$

then, $x \sim \mathcal{C}^+(0, A)$ (Wand et al. [2011]) with $\mathcal{IG}(\cdot, \cdot)$ being the inverse-gamma distribution with probability density function

$$p(z|\alpha, \beta) = \frac{\beta^\alpha}{\Gamma(\alpha)} z^{-\alpha-1} \exp\left(-\frac{\beta}{z}\right), \quad z > 0. \quad (\text{S } 4.4)$$

The above decomposition results in the following revised horseshoe hierarchy

$$\begin{aligned} \omega_{jk} | \lambda_{jk}^2, \tau^2 &\sim \mathcal{N}(0, \lambda_{jk}^2 \tau^2), \\ \lambda_{jk}^2 | \nu_{jk} &\sim \mathcal{IG}(1/2, 1/\nu_{jk}), \\ \tau^2 | \varepsilon &\sim \mathcal{IG}(1/2, 1/\varepsilon), \\ \nu_{12}, \dots, \nu_{p-1p}, \varepsilon &\sim \mathcal{IG}(1/2, 1). \end{aligned} \quad (\text{S } 4.5)$$

Note that it becomes straightforward to construct a Gibbs sampling scheme. The conditional posterior distribution of the edge parameters ω_{jk} is given by

$$(\omega_{jk} | \boldsymbol{\Omega}_{-(jk)}, \mathcal{Y}) \sim N\left(-\frac{b_{jk}}{a_{jk}}, \frac{1}{na_{jk}}\right), \quad 1 \leq j < k \leq p. \quad (\text{S } 4.6)$$

with,

$$a_{jk} = s_{jj} + s_{kk} + \frac{1}{n\lambda_{jk}^2\tau^2}, \quad b_{jk} = \boldsymbol{\Omega}'_{-jk} \mathbf{S}_{-jj} + \boldsymbol{\Omega}'_{-kj} \mathbf{S}_{-kk},$$

the conditional posterior probabilities of the local and global hyperparameters are inverse-gamma distributions

$$\begin{aligned} \lambda_{jk}^2 | \cdot &\sim \mathcal{IG}\left(1, \frac{1}{\nu_{jk}} + \frac{\omega_{jk}^2}{2\tau^2}\right), \\ \tau^2 | \cdot &\sim \mathcal{IG}\left(\frac{1}{2} + \frac{p(p-1)}{4}, \frac{1}{\varepsilon} + \sum_{j=1}^{p-1} \sum_{k=j+1}^p \frac{\omega_{jk}^2}{2\lambda_{jk}^2}\right). \end{aligned} \quad (\text{S } 4.7)$$

Finally, the conditional posterior distribution for the auxiliary variables is given by

$$\begin{aligned} \nu_{jk} | \cdot &\sim \mathcal{IG}\left(1, 1 + \frac{1}{\lambda_{jk}^2}\right) \\ \varepsilon | \cdot &\sim \mathcal{IG}\left(1, 1 + \frac{1}{\tau^2}\right). \end{aligned} \quad (\text{S } 4.8)$$

The resulting Gibbs sampler is summarized in the following algorithm.

Algorithm 2 Entry Wise Gibbs Sampler for BHSC

```
procedure BHSC( $\mathbf{y}_1, \dots, \mathbf{y}_n$ ) ▷ Input the data
  for  $j = 1, \dots, p - 1$  do
    for  $k = j + 1, \dots, p$  do
       $a_{jk} \leftarrow s_{jj} + s_{kk} + \frac{1}{n\lambda_{jk}\tau^2}$ 
       $b_{jk} \leftarrow \boldsymbol{\Omega}'_{-jk}\mathbf{S}_{-jj} + \boldsymbol{\Omega}'_{-kj}\mathbf{S}_{-kk},$ 
       $\omega_{jk} \sim N\left(-\frac{b_{jk}}{a_{jk}}, \frac{1}{na_{jk}}\right)$ 
       $\lambda_{jk}^2 | \cdot \sim \mathcal{IG}\left(1, \frac{1}{\nu_{jk}} + \frac{\omega_{jk}^2}{2\tau^2}\right)$ 
       $\tau^2 | \cdot \sim \mathcal{IG}\left(\frac{1}{2} + \frac{p(p-1)}{4}, \frac{1}{\varepsilon} + \sum_{j=1}^{p-1} \sum_{k=j+1}^p \frac{\omega_{jk}^2}{2\lambda_{jk}^2}\right)$ 
       $\nu_{jk} | \cdot \sim \mathcal{IG}\left(1, 1 + \frac{1}{\lambda_{jk}^2}\right)$ 
       $\varepsilon | \cdot \sim \mathcal{IG}\left(1, 1 + \frac{1}{\tau^2}\right)$ 
    end for
  end for
  for  $j = 1, \dots, p$  do
     $\omega_{jj} \leftarrow \frac{-(\lambda + n\boldsymbol{\Omega}'_{-jj}\mathbf{S}_{-jj}) + \sqrt{(\lambda + n\boldsymbol{\Omega}'_{-jj}\mathbf{S}_{-jj})^2 + 4n^2s_{ii}^k}}{2ns_{ii}^k}$ 
  end for
  return  $\boldsymbol{\Omega}$  ▷ Return  $\boldsymbol{\Omega}$ 
end procedure
```

S 5 Appendix E: Background on the CONCORD regression based generalized likelihood

Let $\mathcal{Y} := (\{\mathbf{y}_i\}_{i=1}^n)$ denote *i.i.d* observations from a p -variate (continuous) distribution, with mean $\mathbf{0}$ and covariance matrix $\boldsymbol{\Omega}^{-1}$. Let \mathbf{S} denote the sample covariance matrix of the observations. In the frequentist setting, one of the standard methods to achieve a sparse estimate of $\boldsymbol{\Omega}$ is to minimize an objective function, comprising of the (negative) Gaussian log-likelihood and an ℓ_1 -penalty term for the off-diagonal entries of $\boldsymbol{\Omega}$, over the space of positive definite matrices. Equivalently, one can maximize the following weighted Gaussian likelihood:

$$\exp\left(-\frac{n}{2}\left\{\text{tr}(\boldsymbol{\Omega}\mathbf{S}) - \log \det \boldsymbol{\Omega} + \frac{\lambda}{n} \sum_{1 \leq j \leq k \leq p} |\omega_{jk}|\right\}\right). \quad (\text{S } 5.1)$$

This approach and its variants are known as the *graphical lasso*, see Yuan and Lin [2007], Friedman et al. [2008], Banerjee et al. [2008]. The function in (S 5.1) can also be regarded as the posterior density of $\boldsymbol{\Omega}$ (up to proportionality) under Laplace priors for the off-diagonal entries, leading to a Bayesian inference and analysis framework Wang et al. [2012]. Note that the requirement on $\boldsymbol{\Omega}$ being positive definite translates to the need of inverting $(p-1) \times (p-1)$ matrices in each iteration of the graphical lasso or Bayesian Markov Chain Monte Carlo (MCMC) based algorithms. This issue is mitigated in the graphical lasso algorithm by the small number of iterations required, but becomes critical for Bayesian approaches that

require many iterations (in the thousands) of the corresponding MCMC scheme.

To address this problem in the frequentist setting, several works (see Peng et al. [2009], Khare et al. [2015]) have considered replacing the Gaussian likelihood by a regression based generalized likelihood. Note that $-\frac{\omega_{jk}}{\omega_{jj}}$ is the regression coefficient of \mathbf{y}_k : when we regress \mathbf{y}_j : on all other variables, and $\frac{1}{\omega_{jj}}$ is the residual variance. This is true even in non-Gaussian settings. Peng et al. [2009] use this interpretation to define a generalized likelihood in terms of the (negative) exponent of the combined weighted squared error loss associated with all these regressions (corresponding to all p variables) as follows.

$$\exp \left(- \sum_{j=1}^p \omega_{jj} \left\{ \sum_{i=1}^n \left(y_{ij} - \sum_{k \neq j} -\frac{\omega_{jk}}{\omega_{jj}} y_{ik} \right)^2 \right\} - \sum_{j=1}^p \frac{n}{2} \log \omega_{jj} \right). \quad (\text{S } 5.2)$$

Under Gaussianity, the expression in (S 5.2) corresponds to the product of the conditional densities of each variable given all the other variables in the data set, and corresponds to Besag Besag [1975]’s pseudo-likelihood. Peng et al. [2009] develop the SPACE algorithm which obtains a sparse estimator for $\mathbf{\Omega}$ by minimizing an objective function consisting of the (negative) log generalized likelihood and an ℓ_1 penalty term for off-diagonal entries of $\mathbf{\Omega}$. However, this objective function is not jointly convex, which can lead to serious convergence issues for the corresponding minimization algorithm.

Khare et al. [2015] address this issue by appropriately re-weighting each of the p regression terms in the exponent of (S 5.2) and combining it with an ℓ_1 penalty term to obtain a regression based loss function which is jointly convex in the elements of $\mathbf{\Omega}$. This loss function, referred by Khare et al. [2015] as the CONCORD objective function, is given by

$$\begin{aligned} Q_{con}(\mathbf{\Omega}) &= -n \sum_{j=1}^p \log \omega_{jj} + \frac{1}{2} \sum_{j=1}^p \sum_{i=1}^n \left(\omega_{jj} y_{ij} + \sum_{k \neq j} \omega_{jk} y_{ik} \right)^2 + \lambda \sum_{1 \leq j < k \leq p} |\omega_{jk}| \\ &= -n \sum_{j=1}^p \log \omega_{jj} + \frac{n}{2} \text{tr}(\mathbf{\Omega}^2 \mathbf{S}) + \lambda \sum_{1 \leq j < k \leq p} |\omega_{jk}|, \end{aligned} \quad (\text{S } 5.3)$$

where \mathbf{S} denotes the sample covariance matrix. The joint convexity of Q_{con} can be used to show that a coordinate-wise minimization algorithm always converges to a global minimum. Note that both Peng et al. [2009] and Khare et al. [2015] relax the parameter space of $\mathbf{\Omega}$ from positive definite matrices to symmetric matrices with positive diagonal entries. The primary purpose of this relaxation is computational. Combined with the quadratic nature of the objective function, this relaxation leads to an *order of magnitude decrease in computational complexity* as compared to graphical lasso based approaches. Note that given the $\log \det \mathbf{\Omega}$ term in the Gaussian likelihood, such a parameter relaxation will not work for the graphical lasso.

While the resulting minimizer may not be positive definite, its sparsity structure can be used to address the primary goal/challenge of selecting the sparsity pattern in $\mathbf{\Omega}$. Khare et al. [2015] establish high-dimensional sparsity selection consistency of this approach, and also demonstrate that the CONCORD approach can outperform graphical lasso when the underlying data is not generated from a multivariate Gaussian distribution. This robustness

is somewhat expected, since the regression based interpretation of Ω does not depend on normality.